

Review

# Recovery of $V_2O_5$ from Spent Vanadium Catalysts: Materials Insights into Deactivation and Recycling Strategies

Sebastian Drużyński \*, Adriana Wróbel-Kaszanek , Bartłomiej Igliński , Urszula Kielkowska   
and Krzysztof Mazurek \*

Faculty of Chemistry, Nicolaus Copernicus University in Toruń, ul. Gagarina 7, 87-100 Toruń, Poland; adriana@umk.pl (A.W.-K.); iglinski@chem.umk.pl (B.I.); ulak@umk.pl (U.K.)

\* Correspondence: sebdru@umk.pl (S.D.); k.mazurek@umk.pl (K.M.)

## Abstract

The growing demand for vanadium and the environmental threat associated with spent catalyst masses have sparked widespread scientific interest in the recovery of  $V_2O_5$  from deactivated vanadium-based catalysts, including those used in sulphuric(VI) acid production. This review places vanadium(V) recovery in the broader context of resource efficiency and the circular economy. The main deactivation mechanisms are analysed, including poisoning, sintering, and structural changes affecting catalytic activity and vanadium availability. Hydrometallurgical approaches to vanadium recovery are discussed, with a particular focus on leaching agents, vanadium speciation in aqueous media, and subsequent separation techniques such as adsorption, solvent extraction, and vanadium(V) precipitation. Key process parameters influencing recovery efficiency, including temperature, pH, and caustic composition, are discussed to provide a comparative assessment of existing methods. The analysis highlights the advantages and limitations of current recovery methods and identifies gaps related to selectivity, process integration, and environmental impact. Overall, the study demonstrates that effective  $V_2O_5$  recovery requires a thorough understanding of catalyst deactivation and solution chemistry. It also outlines models for developing more sustainable and economically viable recycling strategies.

**Keywords:** vanadium catalyst;  $V_2O_5$  recovery; sulphuric(VI) acid production; catalyst deactivation; leaching; adsorption; precipitation; extraction; separation; recovery

## 1. Introduction

Vanadium(V) oxide can no longer be regarded as a conventional transition metal oxide. It is increasingly recognised as a material bridging traditional industrial chemistry and next-generation technologies. Within the classical large-scale chemical industry, vanadium(V) oxide has, for decades, remained an active component of oxidation catalysts. In the domain of emerging technologies, this compound functions as a redox-active material characterised by well-developed surface chemistry, a layered structure, and the ability to couple electron-transfer processes with radiation absorption. This dual role—as both a conventional catalyst and an advanced functional material—means that vanadium(V) oxide should now be considered not only in terms of catalytic activity, but also with respect to raw material security, materials design, and the circular economy [1–8].

The significance of vanadium(V) oxide arises from the intrinsic nature of vanadium chemistry itself. This element is capable of stabilising multiple oxidation states, and the  $V^{5+}/V^{4+}$  and  $V^{4+}/V^{3+}$  redox couples facilitate rapid electron-transfer processes that are



Academic Editor: Guido Busca

Received: 15 May 2026

Revised: 29 May 2026

Accepted: 3 June 2026

Published: 5 June 2026

**Copyright:** © 2026 by the authors.

Licensee MDPI, Basel, Switzerland.

This article is an open access article distributed under the terms and conditions of the [Creative Commons Attribution \(CC BY\) license](https://creativecommons.org/licenses/by/4.0/).

essential both for heterogeneous catalysis and for energy storage applications. Vanadium(V) oxide, as the most widely utilised industrial form of vanadium, combines relatively high thermodynamic stability with a pronounced ability to accommodate ionic intercalation and defect engineering, as well as the presence of a band gap enabling activation under irradiation. In the recent scientific literature, it is precisely this combination of properties that is identified as the principal reason why vanadium(V) oxide remains a material with an exceptionally broad spectrum of applications [3–12]. Its value, therefore, does not stem from any single property, but rather from a rarely encountered capability to operate across multiple functional domains: catalytic, electrochemical, photocatalytic, optoelectronic, and sensing systems—Figure 1.

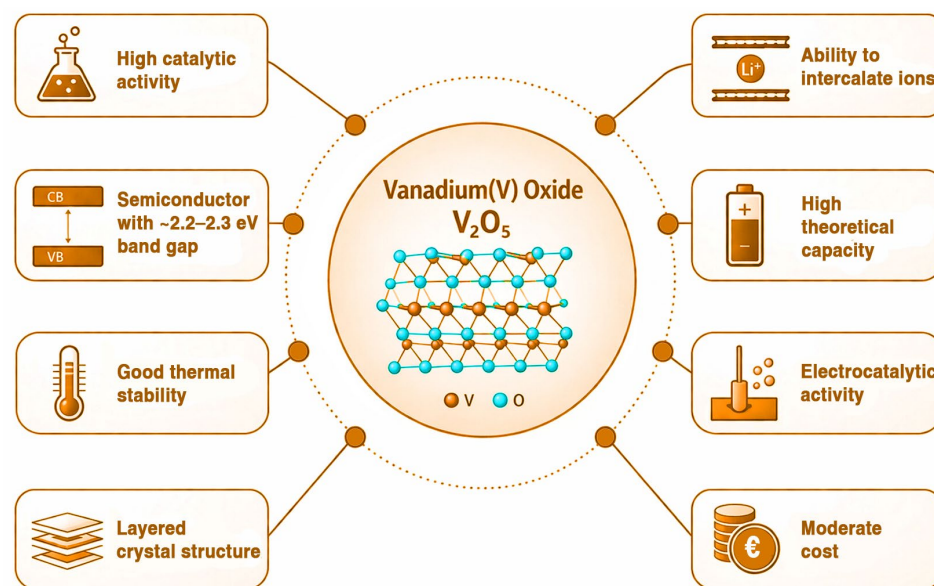


**Figure 1.** Properties of vanadium(V) oxide.

In industrial applications, vanadium(V) oxide remains primarily a catalytic material. The most classical example is the industrial oxidation step of sulphur(IV) oxide to sulphur(VI) oxide in the production of sulphuric(VI) acid, in which vanadium-based catalytic systems replaced the platinum catalyst patented by Peregrine Phillips in 1831, owing to a more favourable balance between activity, resistance to poisoning, and production cost [13–16]. Vanadium(V) oxide-based catalysts are also of considerable importance in the selective catalytic reduction of nitrogen oxides, where systems such as  $V_2O_5$ - $WO_3$ / $TiO_2$  enable efficient reduction of  $NO_x$  with ammonia over a broad temperature range. These catalysts are widely applied, among others, in the treatment of flue gases from power generation and industrial installations [17–20].

From the perspective of materials chemistry, the importance of vanadium(V) oxide extends well beyond its classical industrial applications. In recent years, it has been intensively investigated as a component and precursor of catalytic and electrocatalytic materials (including those for the hydrogen and oxygen evolution reactions), as well as a constituent of photocatalytic and sensing systems [21–24]. An increasing role is also observed in electrochemistry, where its layered crystal structure, enabling cation intercalation, allows its application as an electrode material in supercapacitors and in lithium- and zinc-based batteries [25–27]. Moreover, vanadium(V) oxide is being explored in the context of gas sensors, in which its surface activity and compositional tunability enable improvements in sensitivity and selectivity. It is likewise considered for use in electrochromic and optoelectronic materials, where reversible redox transformations and ion transport within the oxide structure play a crucial role [28,29]. Its photocatalytic

properties are also gaining increasing attention, arising from the presence of a band gap and the ability to generate and separate charge carriers under irradiation. Consequently, vanadium(V) oxide finds application in advanced oxidation processes (AOPs), including the degradation of persistent organic pollutants such as antibiotics, pharmaceuticals, and dyes present in aqueous effluents [30–32].

This multiplicity of applications implies that vanadium(V) oxide cannot be regarded as a niche raw material. Rather, it is a material whose importance is increasing in parallel across several technological sectors; consequently, any loss of the resource, including that occurring in waste streams, is becoming progressively less acceptable from both economic and environmental perspectives. This conclusion gains particular significance in light of the current raw materials situation. Within the European Union, vanadium remains listed as both a critical and a strategic raw material, reflecting not only its technological importance but also the associated supply risks [1,33,34]. Data from the United States Geological Survey indicate that contemporary vanadium production relies not only on primary sources, such as vanadium-bearing titanomagnetites and black shales, but also to a considerable extent on secondary and by-product resources, including steelmaking slags, fly ash, petroleum residues, and spent catalysts [2]. Analysis of production trends presented in Figure 2 shows that, following a relatively stable level during the first decade of the 21st century, global vanadium production has increased markedly after 2015, reaching in recent years levels exceeding 100 thousand Mg per year (expressed as V) and approaching approximately 120 thousand Mg in 2024 [2,35–40]. This growth has been gradual, albeit punctuated by short-term fluctuations, reflecting the strong linkage of the vanadium market to conditions in the steel sector and the concentration of production within a limited number of countries. At the same time, the growing demand for vanadium arises from several overlapping factors, most notably its dominant role in the steel industry, as well as the development of energy storage technologies, in particular vanadium redox flow batteries (VRFBs). This occurs alongside the sustained importance of catalytic and chemical applications, which, combined with supply concentration, further reinforces the role of recovery from secondary sources in the context of resource security and environmental pressures [1–3,41,42].

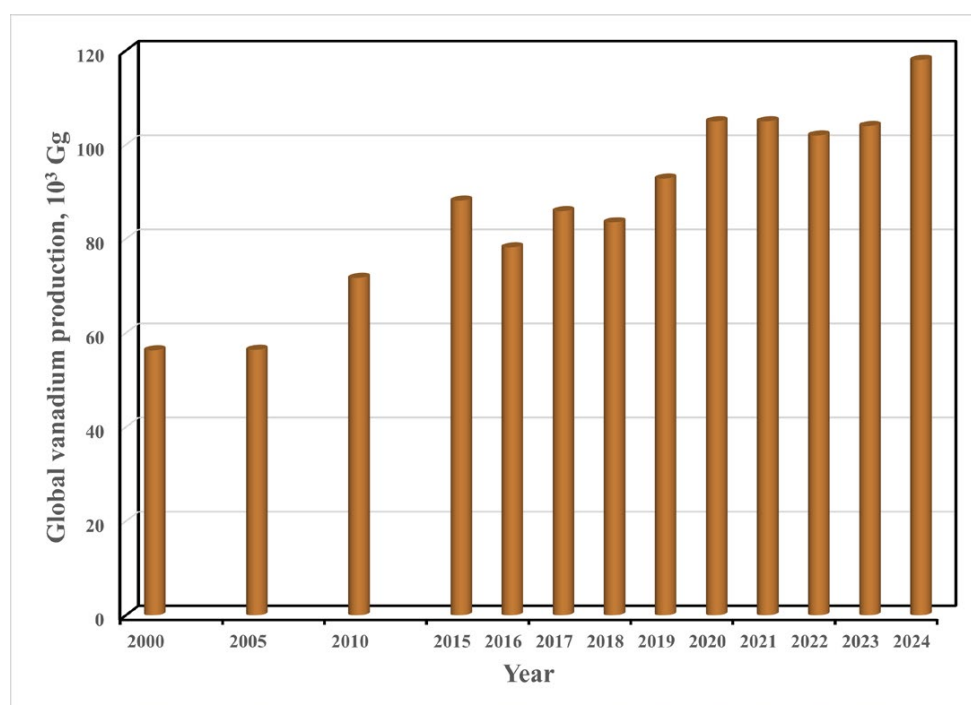


**Figure 2.** Trends in global vanadium production over the period 2000–2024.

In this context, spent vanadium catalysts used in the production of sulphuric(VI) acid can no longer be regarded solely as technological waste, but instead acquire the status of a secondary raw material of significant material value. Reports from recent years indicate that such materials may contain several percent of vanadium(V) oxide, which depending on composition and availability, renders them a competitive source of vanadium relative to certain primary ores [2,43–45]. It should be emphasised, however, that the significance of these materials does not arise exclusively from their vanadium content. Spent catalysts reflect their operational history, including, *inter alia*, the accumulation of impurities, migration of alkaline components, phase transformations, and degradation of the support. Consequently, the efficiency of recovery processes, such as leaching and separation, is governed not only by the chemical composition but also by the form in which vanadium occurs and its distribution within the material structure. For this reason, contemporary approaches to the recovery of vanadium(V) oxide should focus not merely on the total vanadium content, but rather on its chemical speciation and process accessibility [43–45].

In light of the relationships outlined above, encompassing the broad spectrum of applications of vanadium(V) oxide, its growing technological importance, as well as supply and environmental constraints, this material should be regarded as strategic in a dual sense. On the one hand, it remains essential for both traditional chemical process technologies and emerging electrochemical systems; on the other, it exposes the limitations of a model based predominantly on primary raw materials. From this perspective, the transition from a linear model of catalyst use to a concept based on the circulation of functional vanadium-containing materials represents a natural extension of the materials-oriented approach, while simultaneously providing a fundamental rationale for research into the recovery of vanadium(V) oxide from spent catalysts used in the oxidation of sulphur(IV) oxide. Recovery should therefore no longer be viewed as the final stage of waste management, but rather as an integral element in the design of more resilient, selective, and resource-secure chemical technologies, aligned with the principles of green chemistry and the circular economy [1–3,41–45].

## 2. Sulphuric Acid Production and Vanadium-Based Catalysts: Process and Technological Background

Sulphuric(VI) acid is one of the most important large-volume products of inorganic chemistry and has long been regarded as an indicator of industrial development because of its central role in numerous technological processes. According to available literature data, global sulphuric(VI) acid production at the turn of the second and third decades of the twenty-first century amounted to approximately 240–250 million Mg per annum [46,47]. In recent years, this value has likely increased moderately owing to the growing global sulphur supply. Data published by the United States Geological Survey indicate that sulphur production increased from approximately 79–80 million Mg in 2019 to around 84–90 million Mg in 2024–2025 [48,49], suggesting that current sulphuric(VI) acid production may be estimated at approximately 255–270 million Mg annually.

The fertiliser industry remains the dominant consumer of sulphuric(VI) acid, accounting for around 50% of global consumption [50,51]. Sulphuric(VI) acid is primarily used for phosphoric(V) acid production and the manufacture of phosphate fertilisers, making its demand strongly linked to agricultural intensification, food production, and global demographic trends [47,52,53].

Another major application of sulphuric(VI) acid is in the metallurgical industry, particularly hydrometallurgy, where it is used for the leaching of non-ferrous metal ores such as copper, zinc, and nickel. Sulphuric(VI) acid is also widely used in electrochemical refining processes as an electrolyte component enabling high-purity metal recovery [53–56].

Additional important applications include petroleum refining and petrochemical processes, particularly alkylation and purification of petroleum fractions, as well as the manufacture of pigments, dyes, synthetic fibres, and pulp and paper products [57–60]. In recent years, the role of sulphuric(VI) acid has further increased in technologies related to the energy transition and environmental protection, including lithium-ion battery materials, battery recycling, and industrial gas and wastewater treatment. Growing demand for critical metals such as Li, Co, and Ni further strengthens the importance of hydrometallurgical applications of H<sub>2</sub>SO<sub>4</sub> in the low-carbon economy [61–64].

Given the broad industrial importance of sulphuric(VI) acid, the development of efficient large-scale production technologies has been of key significance, progressing from the chamber process to the currently dominant contact process [65–69].

The earliest references to sulphuric(VI) acid date back to the eighth century. However, for many centuries, no efficient production method was developed because of the complexity of sulphur combustion and the slow oxidation of sulphur(IV) oxide to sulphur(VI) oxide [65–69].

The first industrial-scale process was the lead chamber method introduced by John Roebuck in 1746. Subsequent modifications improved nitrogen oxide recovery and overall process efficiency, allowing the method to dominate sulphuric(VI) acid production for nearly two centuries [65–69].

A major breakthrough occurred in 1831 when Peregrine Phillips patented the contact process for the catalytic oxidation of sulphur(IV) oxide to sulphur(VI) oxide. Its industrial implementation was delayed until the late nineteenth century because of catalyst limitations and the sensitivity of the process to gas impurities [65–69]. Despite prolonged competition from the chamber process, the contact process gradually became dominant owing to its higher efficiency, lower environmental impact, and the possibility of producing concentrated sulphuric(VI) acid and oleum [65–69].

Initially, the contact process employed platinum catalysts with high catalytic activity. However, their use was limited by high cost and sensitivity to impurities. A major breakthrough occurred with the introduction of vanadium-based catalysts, characterised by high activity, improved resistance to poisoning, and lower operational costs, which enabled the widespread industrial application of the contact process [65–69].

Modern sulphuric(VI) acid production is based on the catalytic oxidation of SO<sub>2</sub> to SO<sub>3</sub>; therefore, maintaining an appropriate SO<sub>2</sub>-containing process gas stream is essential. Depending on the raw materials and process conditions, SO<sub>2</sub> may be generated by sulphur combustion, roasting of metal sulphides, combustion of H<sub>2</sub>S containing gases, regeneration of spent acids, pyrite combustion, or thermal decomposition of sulphates, in accordance with BAT recommendations and industrial practice [70–72].

Regardless of the source of sulphur(IV) oxide, industrial sulphuric(VI) acid production is carried out in either single contact/single absorption (SC/SA) or double contact/double absorption (DC/DA) systems [65–73]. In SC/SA systems, oxidation and absorption occur in a single cycle, resulting in lower SO<sub>2</sub> conversion and higher emissions. A schematic diagram of this configuration is shown in Figure 3. Typical SO<sub>2</sub> conversion reaches approximately 98–99%, depending on process conditions and catalyst type [65–73].

Modern plants predominantly employ DC/DA systems, in which intermediate SO<sub>3</sub> absorption after the first contact stage shifts the reaction equilibrium towards further SO<sub>3</sub> formation. This configuration enables overall SO<sub>2</sub> conversion levels of approximately 99.5–99.6% while significantly reducing atmospheric emissions, making it the current industrial standard [65–73].

Before catalytic oxidation, the process gas must be purified and dried to remove dust, arsenic compounds, and water vapour that may deactivate the vanadium catalyst. Gas

conditioning is commonly performed using sulphuric acid scrubbers and electrostatic precipitators [65–73].

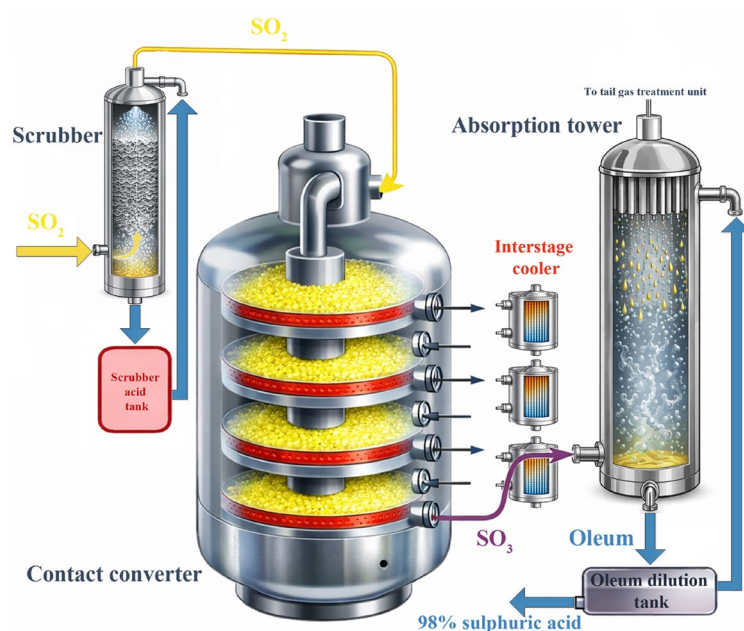


**Figure 3.** Schematic diagram of the contact-absorption section of sulphuric(VI) acid production based on the SC/SA system.

In both SC/SA and DC/DA systems, the key process unit is the vertical multi-bed contact reactor containing vanadium catalyst layers, where  $\text{SO}_2$  is catalytically oxidised to  $\text{SO}_3$  [65–73].

The oxidation of  $\text{SO}_2$  to  $\text{SO}_3$  is an exothermic and reversible reaction; therefore, industrial operation requires careful optimisation of temperature, gas residence time, and gas distribution within the catalyst bed to balance reaction kinetics, equilibrium limitations, and reactor stability [65–73].

The final stage of sulphuric(VI) acid production involves  $\text{SO}_3$  absorption in concentrated sulphuric(VI) acid. The efficiency of this process depends mainly on acid concentration, absorber temperature, gas composition, and hydrodynamic conditions, while  $\text{SO}_3$  and acid aerosol emissions are influenced by absorber operating conditions and mist separation efficiency [65–73].

Industrial  $\text{SO}_2$  oxidation is carried out almost exclusively using vanadium-based catalysts, which replaced platinum systems because of their lower cost and greater resistance to process gas impurities. Modern contact catalysts are based on vanadium(V) oxide supported on porous carriers and promoted with alkali metal sulphates, particularly potassium, sodium, and, in advanced formulations, caesium [65–73].

In industrial practice, vanadium catalysts are predominantly supported on silica-based materials because of their high thermal stability, chemical resistance, and favourable pore structure, which promotes efficient gas diffusion. Silicate materials containing additional stabilising components are also used, whereas alumina-based supports are less suitable owing to sulphate formation under operating conditions [65–73].

Catalyst performance depends not only on chemical composition but also on textural and mechanical properties, including pore structure, strength, and resistance to abrasion. Equally important is the catalyst geometry, which is optimised to balance catalytic activity and gas flow resistance. Industrial reactors commonly employ different catalyst types in successive beds, with upper layers designed for higher thermal and impurity resistance

and lower layers containing more active, often caesium-promoted, catalysts. Typical shapes of industrial vanadium catalysts are presented in Figure 4 [65–73].

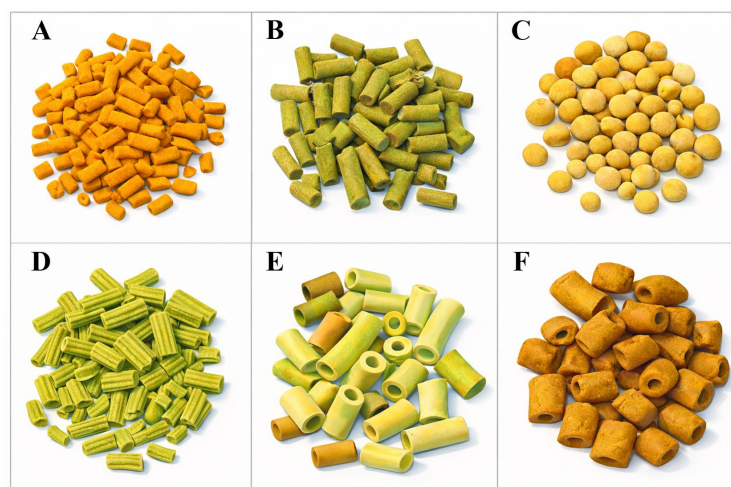


**Figure 4.** Typical geometrical forms of vanadium catalysts used in industrial practice: (A) cylinders, 4 mm diameter; (B) cylinders, 6 mm diameter; (C) spheres; (D) corrugated cylinders, 6 mm diameter; (E) rings, 9/4 mm; (F) rings, 12/5 mm.

Although vanadium catalysts exhibit high operational stability, their activity gradually decreases during long-term operation because of interactions with process gas components and operating conditions. Catalyst deactivation affects SO<sub>2</sub> conversion efficiency and reactor temperature profiles, making it a key issue in sulphuric(VI) acid plant operation [65–73].

### 3. Deactivation of Vanadium Catalysts During the Industrial Oxidation of Sulphur(IV) Oxide

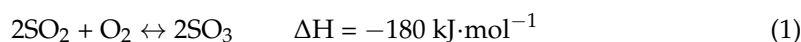
The volume of sulphuric acid production is widely regarded as an indicator of economic development. The catalytic oxidation of sulphur(IV) oxide to sulphur(VI) oxide is the central unit process in the industrial production of sulphuric acid using the contact method. With the introduction of vanadium catalysts in 1915, they became the cornerstone of this technology, replacing the chamber process [74–77]. Despite years of optimisation of catalyst form and composition, vanadium mass deactivation remains unresolved. This issue is one of the most complex challenges in sulphuric acid production. Catalyst degradation is not a homogeneous process; it results from the combined effects of thermal, chemical, and physical factors. These factors permanently reduce catalytic properties, increase hydraulic resistance within the contact apparatus, and raise emissions of sulphur compounds into the atmosphere [74–77].

#### 3.1. The Physicochemical Characteristics of the Active Vanadium Catalyst

Vanadium catalysts used in the contact process are a distinctive class of heterogeneous catalysts. Under operating conditions, the active phase is in a liquid state. This system is called supported liquid phase (SLP) catalysis. The liquid active phase is vanadium pentoxide (V<sub>2</sub>O<sub>5</sub>) dissolved in molten alkali metal disulphates, mainly potassium, and less often sodium or caesium. The support for this chemically active phase is porous silica (SiO<sub>2</sub>). The structure and texture of the silica determine the effective gas-liquid contact surface area [74].

The mechanism of action of the catalyst is based on the vanadium redox cycle, which takes place within vanadium complexes of LK = 4, where SO<sub>2</sub> and oxygen molecules

coordinate with the central ion. The oxidation reaction is shown to proceed according to the general Equation (1).



The activation energy of this process in the absence of a catalyst is so high that the reaction in the gas phase proceeds at a negligible rate. The employment of a vanadium catalyst has been demonstrated to reduce this energy barrier, thereby enabling operation within a temperature range of 400–600 °C. Deviations from the optimal composition of the active phase or disruptions to the support structure have been shown to result in a decrease in activity. This is evidenced by a decline in the conversion rate and an increase in the ignition temperature towards higher values [74–77].

### 3.2. Classification and Mechanisms of Thermal Deactivation

Thermal deactivation is inextricably linked to the high-temperature operating conditions of the contact apparatus. Despite the fact that vanadium catalysts demonstrate elevated thermal stability, protracted exposure to temperatures in excess of 600–620 °C results in irreversible structural alterations [74–77].

### 3.3. Phase Transformations in the Silica Support

The support, which provides the mechanical foundation for the catalyst, undergoes ageing processes that are accelerated by the presence of the liquid phase. In a fresh catalyst, silica is most commonly present in the form of cristobalite. It has been demonstrated that, upon exposure to elevated temperatures, cristobalite undergoes a transformation into quartz. This process is accompanied by a concomitant change in both the grain's density and its internal stresses. The extant literature indicates a critical point at approximately 575 °C, the temperature at which the transition from  $\alpha$ -quartz to  $\beta$ -quartz occurs [74–77]. According to other studies, at a temperature of approximately 575 °C, these alterations become so pronounced that they result in the closure of micro- and mesopores. This process, known as sintering, has been shown to reduce the specific surface area of the catalyst by up to 90%, thereby limiting the availability of the active phase to the reactants [74–77].

### 3.4. The Recrystallisation and Degradation of the Active Phase

These phenomena occur as a consequence of prolonged exposure of the liquid phase of the catalyst. Alkali metal disulphates, which act as a solvent for vanadium, may undergo decomposition when the bed is overheated, resulting in the release of sulphur trioxide and the conversion into solid sulphates ( $\text{K}_2\text{SO}_4$ ). This results in a significant increase in the melting point of the mixture, thereby inducing the crystallisation of the active phase within the pores. This phenomenon renders the catalyst ineffective, as the  $\text{SO}_2$  oxidation reaction occurs efficiently only in the molten phase. At temperatures in excess of 600 °C, vanadium may undergo reduction to inactive forms or stable compounds with metallic impurities, thereby resulting in a permanent reduction in the redox potential of the system [74,78,79].

### 3.5. Chemical Poisoning of Vanadium Catalysts—The Effect of Gaseous Contaminants

The phenomenon of chemical deactivation, which is commonly referred to as poisoning, is the result of interactions between the components of the process gas and the catalyst components. This problem is especially evident in metallurgical plants, where the roasting gas contains a wide range of impurities that cannot be removed in the scrubbing unit [80,81].

Arsenic compounds, and most notably  $\text{As}_2\text{O}_3$ , are regarded as one of the most hazardous substances for platinum contacts. The elevated cost of platinum, in conjunction

with its sensitivity to arsenic, has necessitated the employment of vanadium catalysts. However, even these are not fully resistant to its effects. In the operating conditions of the contact apparatus, arsenic trioxide oxidises to non-volatile  $\text{As}_2\text{O}_5$  (Equation (2)), which reacts with vanadium pentoxide to form stable, inactive complexes of the  $\text{V}_2\text{O}_5 \cdot \text{As}_2\text{O}_5$  type (Figure 5a). These compounds have been shown to impede the active sites and modify the surface tension of the disulphate alloy, resulting in its displacement and the ‘flooding’ of the finest pores in the support material. In addition, arsenic compounds react with the alkaline promoter phase (primarily potassium pyrosulphates), leading to the formation of stable arsenates. This process depletes the alkaline promoter, disturbs the composition and physico-chemical properties of the molten active phase, and consequently reduces oxygen mobility and catalytic activity (Figure 6). The permissible concentration of arsenic in the process gas is strictly limited and is typically below  $1.2 \text{ mg} \cdot \text{m}^{-3}$  [74].



**Figure 5.** Images of used vanadium catalysts: (a) poisoning with arsenic compounds; (b) deactivation caused by dust agglomeration on the surface; (c) the effect of water vapour on the catalyst surface. <http://www.sulphuric-acid.com/Sulphuric-Acid-on-the-Web/home.htm> (28 April 2026; 13:30).

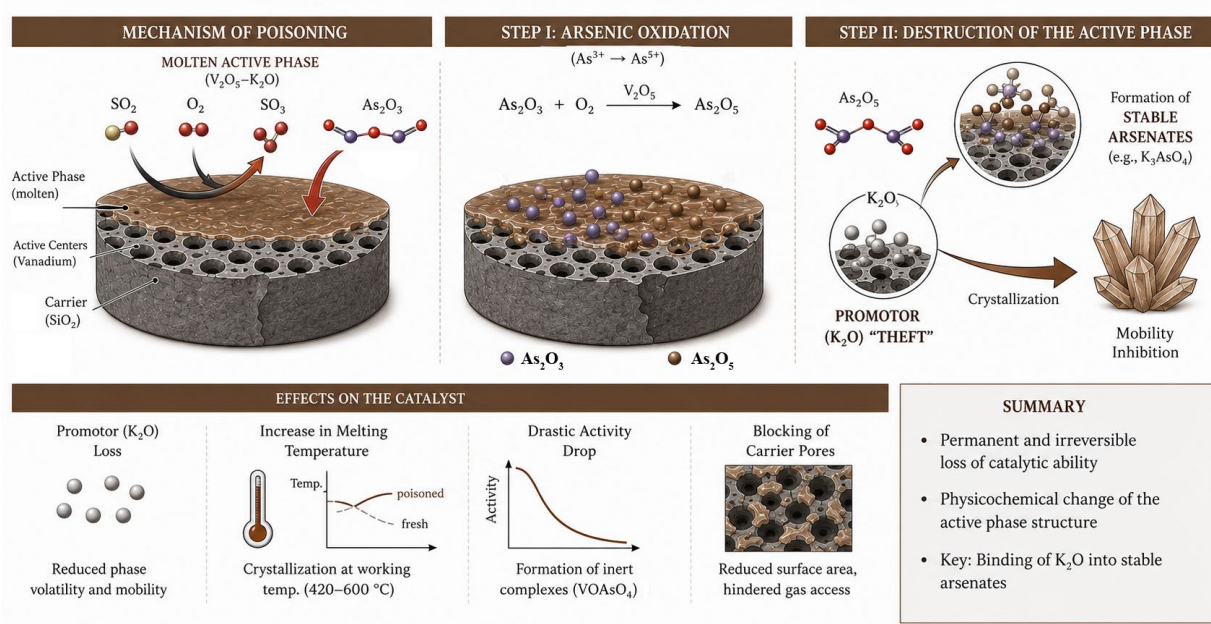
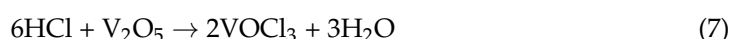
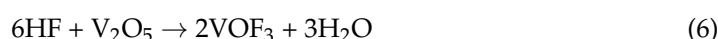
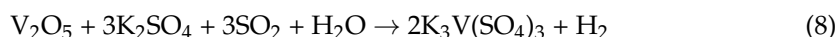


**Figure 6.** Scheme of the mechanism of  $\text{As}_2\text{O}_3$  interaction with the vanadium catalyst.

Fluorine compounds (HF, SiF<sub>4</sub>) and chlorine compounds (HCl, Cl<sub>2</sub>) have been observed to exhibit a dual deactivation mechanism. In one instance, they react with silica, forming volatile silicon tetrafluoride (SiF<sub>4</sub>) (Equation (3)). This process leads to the chemical ‘dissolution’ of the carrier and a significant weakening of the granules’ mechanical properties. Conversely, fluorine and chlorine react with vanadium to form volatile oxyhalides, such as vanadium oxyfluoride (VOF<sub>3</sub>) (Equations (4) and (6)) or vanadium oxychloride (VOCl<sub>3</sub>) (Equations (5) and (7)) [81–83]. This process results in the physical loss of vanadium from the bed—the active phase literally ‘evaporates’ from the reactor, manifesting as a systematic decline in the conversion rate, which cannot be compensated for by adjusting process parameters [81–83].



The presence of moisture in the process gas constitutes a pivotal factor, especially within the lower sections of the bed or during the initiation of the plant. Water vapour has been shown to promote the condensation of sulphuric acid within the catalyst pores, resulting in agglomeration and granule cracking (Figure 5c). Spectroscopic studies (FTIR, XRD) indicate alterations in the oxidation state of vanadium caused by water vapour. In the presence of water, vanadium in the active phase is reduced from V<sup>5+</sup> to V<sup>4+</sup>, and even V<sup>3+</sup> (e.g., in the form of K<sub>3</sub>V(SO<sub>4</sub>)<sub>3</sub>). This phenomenon is characterised by a change in the catalyst’s colour from yellow to bright green. The activity of the reduced forms of vanadium is negligible, leading to a sharp drop in process efficiency [79].



Iron is a distinctive instance of a deactivating agent, as it enters the catalyst from two distinct sources: firstly, from the exterior (dust from ore roasting); and secondly, as a consequence of corrosion processes occurring within the system. The presence of steel corrosion products, primarily iron sulphates, has been observed in the gaseous phase, and these substances subsequently deposit on the surface of the catalyst, inducing a sequence of unfavourable phase transitions [15].

The mechanism of potassium-iron sulphate formation is as follows: iron oxides (Fe<sub>2</sub>O<sub>3</sub>) are introduced into the catalyst in an SO<sub>3</sub>-rich atmosphere (Figure 7). Sulphation then occurs. The principal product of this reaction is potassium-iron double sulphate, KFe(SO<sub>4</sub>)<sub>2</sub> (Equation (9)). This process is particularly deleterious due to the concomitant increase in volume. The process of crystallisation of hard sulphate sinter within the silica pores of the material generates mechanical stresses which exceed the strength of the support. This phenomenon, termed ‘pore bursting’, has been observed to result in the rapid crumbling of the catalyst and the formation of significant quantities of fines [73,74,81,82,84] (Figure 7). As illustrated in Table 1, the porous structure parameters of the ‘fresh’ and ‘spent’ catalysts are summarised.



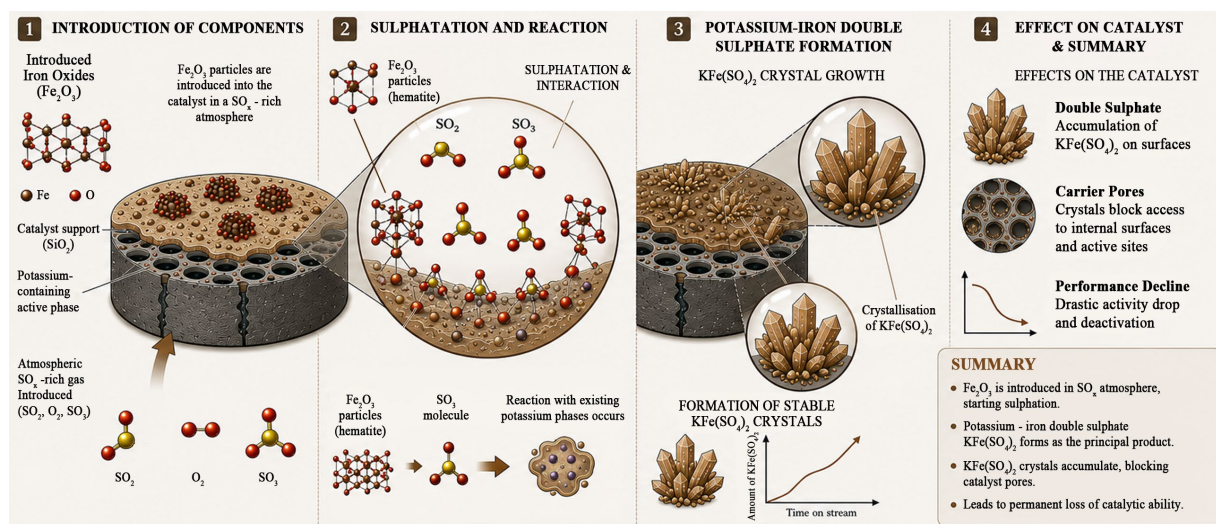


**Figure 7.** Scheme of the mechanism of  $\text{Fe}_2\text{O}_3$  interaction with the vanadium catalyst.

**Table 1.** Change in the porous structure of the vanadium catalyst under the influence of iron compounds and long-term operation [73,74].

Structural Parameter	'Fresh' Catalyst	'Spent' Catalyst
Pore volume, $\text{cm}^3 \cdot \text{g}^{-1}$	0.520	0.482
Pore radius, $\mu\text{m}$	0.51	0.81
Percentage of wide pores ( $>0.81 \text{ mm}$ ), %	7.8	61.9

The data presented in Table 1 unequivocally indicate that iron deactivation changes the catalyst's structure from fine- and medium-porous to macroporous. The presence of iron sulphates during the initial phase of catalyst operation has been shown to increase mechanical strength (formation of a hard crust). However, over a longer period (250 h tests), this presence leads to the complete physical destruction of the grains [73,74,81,82,84].

A notable element of catalyst deactivation is the presence of 'phase iron', defined as iron compounds that are introduced into the system during the recycling of spent vanadium-based catalysts for the production of new catalysts [73,74]. It has been demonstrated that iron derived from recycled vanadium masses exerts a significantly more destructive effect on the catalyst than does pure iron(III) oxide. This phenomenon can be attributed to the inherent defectivity of the phase iron crystal structure, which is inherently bound to potassium. This binding hinders the effective formation of the active disulphate binder within the novel catalyst, thereby compromising its functionality. The production of catalysts in this manner, motivated by cost savings, results in a product with a drastically reduced lifespan [73,74].

### 3.6. Physical Deactivation and Operational Issues

Physical deactivation does not alter the chemical nature of the catalyst. Rather, it prevents the catalyst from functioning properly by creating a mechanical barrier to mass and heat transfer [70,73,74,81,82,84].

- The occurrence of dust accumulation and bed clogging (Figure 5b). Dust particles, such as ash residues from sulphur combustion or metal oxides from calcining furnaces, are carried by the gas and settle within the voids between the catalyst components. This results in the formation of a hard crust, which has been shown to significantly increase hydraulic resistance. The increase in resistance has a direct impact on the power

output of the blowers supplying the gas, which in turn significantly affects electricity costs. In exceptional circumstances, a phenomenon referred to as ‘channelled flow’ occurs, whereby the gas is observed to traverse solely through a limited number of unobstructed channels. Consequently, a marked decline in contact time and a concomitant reduction in the conversion rate are evident [70,73,74,81,82,84].

- Mechanical abrasion and screenings during operation in the contact unit, the catalyst packing (particularly those with complex shapes such as Raschig rings or star-shaped elements) undergoes abrasion due to vibrations and impacts from the gas stream. The resultant catalytic dust further clogs the bed. Statistics from Polish plants (Głogów, Legnica, Police) demonstrate that the proportion of screenings generated during routine inspections ranges from 2% to as much as 15% of the bed mass, contingent on process stability and catalyst quality [70,73,74,81,82,84].

#### 4. Catalyst Condition Diagnostics—Laboratory and Industrial Methods

An accurate diagnosis of the causes of a decline in activity is crucial for determining whether to screen, replenish or completely replace the catalyst bed. Modern diagnostics employ sophisticated instrumental analysis methods [73,74].

The X-ray powder diffraction (XRD) technique is employed to analyse the crystalline structure of materials. The purpose of the study was to examine the morphology and phase composition of the solid phase. This enabled the identification of the crystalline forms of vanadium and the support.

Energy-dispersive X-ray spectroscopy (EDX/EDXRF) is an analytical technique used to obtain the elemental composition of a specimen by measuring the spectrum of X-rays emitted during the process of electron excitation. The instrument is employed for the quantitative and qualitative analysis of elemental composition, with the purpose of identifying vanadium, promoters and impurities, in both solutions and the solid phase. Modern diagnostics employs advanced instrumental analysis methods, including the following.

- Transmission electron microscopy (TEM/HRTEM/HAADF-STEM). This instrument is ideal for structural analysis, including the identification of lattice defects and the dispersion of the active vanadium phase.
- Electron paramagnetic resonance spectroscopy (EPR/ESR) is a technique used in the field of spectroscopy. The present text provides information on the immediate coordination environment of vanadium ions and enables the tracking of catalytic reaction mechanisms.
- Porosimetry is a method of measuring the porosity of a material. One example of this is mercury porosimetry. The assessment of specific surface area, pore volume and density is of crucial importance in determining the availability of active sites.
- The application of UV-Vis spectroscopy is a key element of the research. The composition of solutions is analysed in order to facilitate the study of spent catalysts.
- Thermal analysis (TA) methods. The measurement of changes in mass (TGA) or enthalpy (DSC) as a function of temperature is a method by which the thermal stability of the catalyst can be determined.
- Activity studies in a laboratory setup: Analysis of activity in oxidation processes in the temperature range 400–600 °C.

A noteworthy diagnostic instrument is the methanol oxidation reaction, which functions as a probe for the surface state of a vanadium catalyst. The surface of a fresh catalyst is characterised by a specific balance between redox and acid centres. It has been demonstrated that a deactivated catalyst displays a change in selectivity. In this instance, the selectivity for the oxidation of methanol to formaldehyde has been observed to increase from 8% to 46%, whilst the selectivity for oxidation to CO<sub>2</sub> has been shown to decrease

from 17.8% to just 0.8%. This selectivity profile indicates the dominance of acid sites and the blocking of vanadium's oxidising potential, which is directly correlated with a decrease in SO<sub>2</sub> oxidation activity [74].

## 5. Criteria for the Replacement and Segregation of Vanadium Catalysts, and Innovations in Deactivation Resistance

The decision to take a catalyst out of service is based on what is known as relative deactivation. Notwithstanding the satisfactory level of chemical activity, a decline in mechanical strength that falls below the established limit value for a specific mass (for instance, 10 kg/grain) necessitates replacement, as this may lead to sudden physical destruction and the obstruction of gas flow [73,74,83,84].

The present focus of research into increasing resistance to deactivation is on the creation of catalysts with extended service life by modifying their composition and form. Three principal domains of research can be identified:

The following section will introduce the concept of promoters entering the active phase. During the production process, the introduction of caesium or cerium compounds into the catalyst mass is a possibility. This process has been shown to reduce the ignition temperature (approximately 370–390 °C), thereby enabling operation at a lower temperature on the final shelves of the contact apparatus. This has been shown to reduce thermal stresses and the risk of crystallisation of the active phase [83].

Advanced silica supports. The utilisation of synthetic structures with controlled mesoporosity, in conjunction with the doping of the support with aluminium (Al<sub>2</sub>O<sub>3</sub> or TiO<sub>2</sub>), has been demonstrated to enhance thermal stability and resistance to shrinkage at elevated temperatures [85].

Low-resistance packing: The switch from cylinders to Raschig rings, star-shaped packing or ribbed rings increased the dust-holding capacity and allowed for longer service life even with lower-quality process gas [84].

## 6. Hydrometallurgical Approaches to Vanadium Recovery from Spent Catalysts

In the scientific literature, spent catalysts containing vanadium are classified into three main groups with different physicochemical characteristics [86].

- V<sub>2</sub>O<sub>5</sub>-SiO<sub>2</sub>-K/Na type SVC (Spent Vanadium Catalysts). Spent catalysts from sulphuric acid production plants. Classic contact catalysts in which the active phase consists of V<sub>2</sub>O<sub>5</sub> deposited on a SiO<sub>2</sub> support, usually with the addition of alkali promoters, mainly K<sub>2</sub>SO<sub>4</sub> and Na<sub>2</sub>SO<sub>4</sub> [87].
- SCR (Selective Catalytic Reduction) of the V<sub>2</sub>O<sub>5</sub>-WO<sub>3</sub>/TiO<sub>2</sub> or V-Mo/Ti type. Spent catalysts used in flue gas denitrification processes. In these materials, the active vanadium phase is mainly deposited on TiO<sub>2</sub>, and typical additives include WO<sub>3</sub> or MoO<sub>3</sub> [88].
- HDS-hydrodesulphurisation of the Ni-Mo-V/Al<sub>2</sub>O<sub>3</sub> type. Refinery catalysts in which vanadium is not the primary active component, but occurs as a metallic impurity deposited on an Al<sub>2</sub>O<sub>3</sub> support, usually together with Ni and Mo [89].

SVC-type materials, due to their vanadium content of approximately 5 wt.% and the presence of alkali promoters, are among the most promising feedstocks for its recovery. Knowledge of their specific chemical composition is crucial for optimising recovery processes, as illustrated in Table 2, which shows the average elemental composition of spent contact catalysts.

**Table 2.** Elemental composition of spent vanadium catalysts originating from industrial SO<sub>2</sub> oxidation to SO<sub>3</sub> units used in sulphuric acid production (wt.%).

Country	V	K	Na	Fe	S	Cu	Zn	Pb	Hg	Cd	Si	Rest	Reference
Poland * (sulphur type)	2.98	5.98	N/A	1.19	5.68	<0.01	N/A	N/A	N/A	N/A	N/A	84.17	[90]
Poland * (metallurgical type)	3.04	6.51	N/A	1.61	5.51	1.76	0.16	0.37	<0.03	<0.02	N/A	81.04	[90]
Spain (metallurgical type)	4.04–4.38	6.03–6.86	0.26–0.93	0.70–0.96	6.37–12.5	N/A	N/A	N/A	N/A	N/A	~48.2	~26–33	[91]
Belarus (sulphur type)	7.5	9.1	N/A	1.4	10.2	N/A	N/A	N/A	N/A	N/A	23.2	48.6	[44]
Cuba (metallurgical type)	1.92	N/A	1.09	6.35	7.17	0.014	0.018	0.16	N/A	N/A	30.03	51.68	[92]
China * (metallurgical type)	2.6	8.46	0.79	7.4	21.31	N/A	N/A	N/A	N/A	N/A	23.24	35.39	[93]
Jordan * (sulphur type)	2.974	9.212	0.752	0.690	4.575	0.0039	0.0044	N/A	N/A	N/A	31.724	48.78	[43]

\* Elemental values calculated from the reported oxide composition.

The chemical composition of spent vanadium catalysts originating from the industrial SO<sub>2</sub> oxidation to SO<sub>3</sub> process may vary despite their common technological application in sulphuric acid production. Such variability may be associated with differences in catalyst operating time, degree of deactivation, gas composition, and process history, all of which can influence the physicochemical transformations occurring during long-term industrial operation. In addition, post-operational factors, including storage conditions and environmental exposure, may further affect the composition of the spent catalyst material. In particular, prolonged storage under atmospheric conditions may promote the partial leaching or washing out of selected catalyst components as a result of contact with atmospheric precipitation and moisture. Consequently, the chemical composition of spent catalysts reported in the literature may differ between sources, even for catalysts derived from the same technological process.

The recovery of vanadium from SVC materials is also economically viable. The costs of obtaining vanadium from secondary sources are lower than those of extracting it from primary deposits [94–96]. An important aspect of the V recovery process is its environmental dimension. V<sub>2</sub>O<sub>5</sub> is a more toxic form of vanadium than its compounds in which it occurs as V(IV) and V(III). A deactivated catalyst from H<sub>2</sub>SO<sub>4</sub> production, if improperly stored, can contribute to soil and groundwater contamination, exposing plants, freshwater organisms and humans to its toxic effects [97–100].

The implementation of technologies for recovering metals from spent catalysts leads to a reduction in the flow of hazardous waste and minimises the risk of secondary environmental pollution, which is consistent with the principles of sustainable development and the circular economy [80,101].

The efficiency of hydrometallurgical processes is closely linked to the speciation of vanadium in aqueous solutions (Figure 8), which determines its solubility, mobility and reactivity [102]. The stability of the various chemical forms depends on the pH of the system and the redox potential [94,95]. In an acidic environment, cationic forms such as VO<sup>2+</sup> and VO<sub>2</sub><sup>+</sup> predominate, whereas under alkaline conditions, the anionic form of vanadium(V) in the form of orthovanadate VO<sub>4</sub><sup>3-</sup> and its protonated forms: HVO<sub>4</sub><sup>2-</sup> and H<sub>2</sub>VO<sub>4</sub><sup>-</sup>, predominate. The high stability of these forms is the basis for the efficiency of alkaline leaching. In the intermediate pH range, the formation of more complex polymeric structures is observed, including pyro- and polyvanadates such as V<sub>2</sub>O<sub>7</sub><sup>4-</sup> and V<sub>10</sub>O<sub>28</sub><sup>6-</sup>, the presence of which significantly affects the efficiency of separation processes. Due to

their larger size, different electronic structure or complexation characteristics, vanadium polyanions may limit the efficiency of solvent extraction and exhibit different affinities for the active sites of adsorbents [103–105].

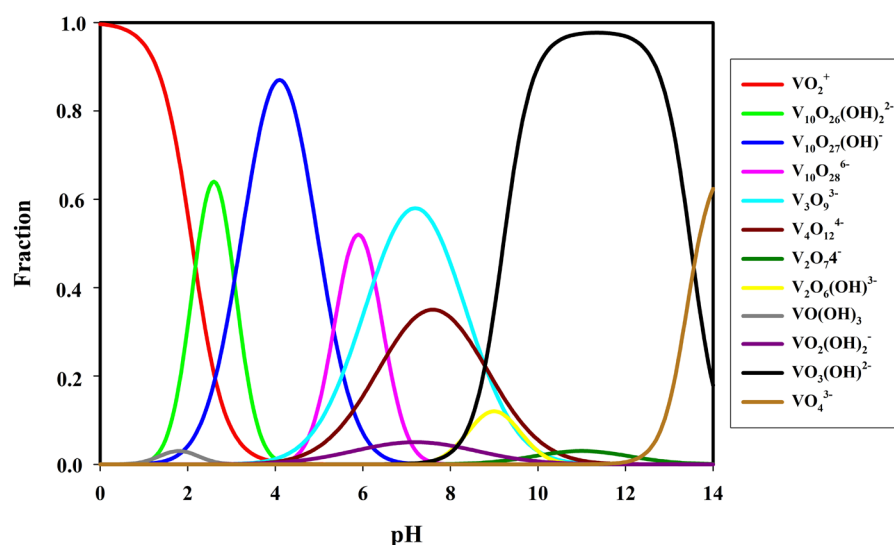


**Figure 8.** Distribution of vanadium species as a function of pH [103–105].

Leaching is a fundamental stage in the hydrometallurgical recovery of vanadium from spent catalysts. The choice of a suitable leaching medium and process conditions directly influences the degree of vanadium leaching and the level of co-extraction of matrix components or catalyst impurities. Achieving 100% leaching of vanadium compounds is impossible due to the presence of poorly soluble aluminium vanadates ( $x\text{Al}_2\text{O}_3 \cdot y\text{V}_2\text{O}_5 \cdot 2\text{H}_2\text{O}$ ) and iron vanadates ( $\text{Fe}_2\text{O}_3 \cdot x\text{V}_2\text{O}_5$ ) in the SVC, and  $\text{Ca}(\text{VO}_3)_2$  in the presence of calcium. This effect is also influenced by the sorption of vanadium compounds on the silica surface, which establishes a practical upper limit for the leaching yield [106,107]. Conventional separation techniques, such as liquid-liquid extraction (including the use of a liquid membrane—SLM), selective precipitation, ion exchange, or adsorption, are used to isolate vanadium from leaching solutions.

The selection of an appropriate vanadium leaching method depends strongly on the chemical composition of the spent catalyst material and the type, as well as the extent of accumulated contaminants. Acidic leaching processes are characterised by high vanadium extraction efficiency; however, they are generally less selective, as significant amounts of accompanying metal impurities, including Fe, Cu, and Zn, may also dissolve into the leachate. In contrast, alkaline leaching is often considered a more selective approach for vanadium recovery, particularly for spent catalysts containing elevated concentrations of metallic contaminants. Under alkaline conditions, vanadium compounds readily form soluble vanadates, whereas many accompanying metal impurities remain in the solid residue. Consequently, the choice of the leaching route should be determined individually depending on the contamination profile, degree of catalyst deactivation, and the intended downstream processing requirements.

### 6.1. Extraction of Vanadium from Spent Vanadium Catalyst Mass

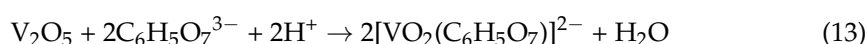
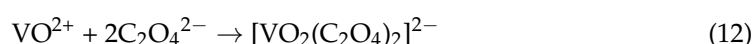
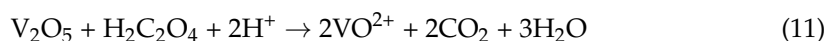
Recovery processes often begin with the activation of the material. Thermal activation (sintering at 500–700 °C) with the addition of fluxes such as  $\text{NaCl}$ ,  $\text{Na}_2\text{CO}_3$  or  $\text{Na}_2\text{SO}_4$  leads to the conversion of poorly soluble vanadium phases into soluble sodium vanadates. High temperatures also promote the transformation of sulphides into oxides and increase the porosity of the silica matrix, which facilitates the diffusion of leaching reagents. The

resulting alloy is leached out using alkaline, acidic or V(II)-containing solutions [108–110]. Additionally, the products of the calcination reaction (including the oxidising effect of chlorine when using NaCl) promote the destruction of the catalyst structure and an increase in vanadium extraction efficiency to over 90%. An alternative is chemical activation carried out using oxidising solutions, such as H<sub>2</sub>O<sub>2</sub>, which leads to partial breakdown of the catalyst structure and increased availability of vanadium-bearing phases for leaching, without the need for high temperatures [93].

A catalyst with a particle size in the range of 0.12–0.2 mm was roasting at 850 °C using a melting agent consisting of NaCl:Na<sub>2</sub>CO<sub>3</sub>:NaNO<sub>3</sub> (15:7.5:2.5/100 parts catalyst) for 3.5 h. The resulting alloy was leached with water, with an S:L ratio of 1:5. A V<sub>2</sub>O<sub>5</sub> recovery of 76% was achieved using four leaching cycles, with the majority of the vanadium being leached out in the first two cycles. However, calcining the catalyst at 450 °C and replacing Na<sub>2</sub>CO<sub>3</sub> in the melt with solid NaOH resulted in a decrease in V<sub>2</sub>O<sub>5</sub> recovery to approximately 45% [90].

### 6.1.1. Acid Leaching

The literature distinguishes several main methods of acid leaching, including media based on H<sub>2</sub>SO<sub>4</sub> and HCl, reductive systems, and solutions of organic acids with complexing capabilities. These systems differ in the dissolution mechanisms of vanadium-bearing phases and in the degree of co-leaching of catalyst matrix components and impurities, which affects their selectivity and process efficiency. Depending on the type of extractant used, several processes occur during leaching in an acidic environment. In general, vanadium(V) oxide reacts according to Equation 10. In the presence of oxalic acid, vanadium(V) is reduced to vanadium(IV), a process that may be accompanied by the formation of oxalate complexes (Equations (11) and (12)). Citric acid, on the other hand, has much weaker reducing properties, so complexation of vanadium ions is the dominant mechanism (Equation (13)).



A comparison of exemplary acid leaching systems used for vanadium oxide-containing catalysts, process conditions, and vanadium recovery yields is presented in Table 3.

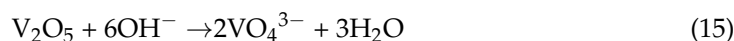
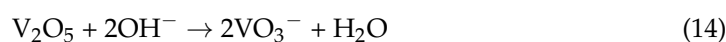
**Table 3.** Acid leaching systems for vanadium recovery from spent catalysts.

Acid Leaching System	Conditions (C, T, Time, L/S, Particle Size)	V Recovery from PLS (%)	Reference
HCl	2 mol·dm <sup>-3</sup> , room temperature, <10 min, 2.5 cm <sup>3</sup> ·g <sup>-1</sup> , particle size 2–4 mm	~99	[111]
H <sub>2</sub> SO <sub>4</sub>	0.5 mol·dm <sup>-3</sup> , 25 °C, 5 min, 5 cm <sup>3</sup> ·g <sup>-1</sup> , particle size 0.00252–0.00397 mm	91, 96	[112]
H <sub>2</sub> C <sub>2</sub> O <sub>4</sub> (oxalic acid)	2 wt.%, 50 °C, 4 h, 10–25 cm <sup>3</sup> ·g <sup>-1</sup> , particle size < 0.250 mm	~90	[74]
C <sub>6</sub> H <sub>8</sub> O <sub>7</sub> (citric acid)	10 wt.%, 50 °C, 4 h, >10 cm <sup>3</sup> ·g <sup>-1</sup> , particle size < 0.160 mm	~90	[113]
C <sub>6</sub> H <sub>8</sub> O <sub>7</sub> + H <sub>2</sub> O <sub>2</sub> (citric acid)	0.1 mol·dm <sup>-3</sup> C <sub>6</sub> H <sub>8</sub> O <sub>7</sub> , 0.1 mol·dm <sup>-3</sup> H <sub>2</sub> O <sub>2</sub> , 50 °C, 2 h, 25 cm <sup>3</sup> ·g <sup>-1</sup> , particle size < 0.150 mm	95	[114]

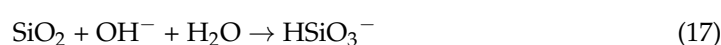
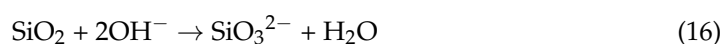
The use of a hot 90 °C HCl solution as a leaching agent allows for higher metal recoveries (~99%), including vanadium, compared to sulphuric(VI) acid leaching. However, its practical application is limited by the high corrosiveness of the chloride environment, which significantly increases equipment material requirements and process costs [115]. Analysis of the presented acid leaching systems indicates that H<sub>2</sub>SO<sub>4</sub> based solutions are the most widespread and industrially mature extraction media for vanadium recovery, providing a high degree of extraction with moderate selectivity toward accompanying metals. One of the proposed methods for vanadium recovery from SVC consists of a two-stage leaching process. First, a H<sub>2</sub>SO<sub>4</sub> solution (pH 1.2–1.3) is applied with ultrasound assistance for 5 min. In the second stage, a 0.01 mol·dm<sup>-3</sup> Na<sub>2</sub>SO<sub>3</sub> solution is used (15 min, ambient temperature), achieving a vanadium leaching yield of 98 wt.% [44]. On the other hand, the application of 8 mol·dm<sup>-3</sup> H<sub>2</sub>SO<sub>4</sub> with a minor addition of ascorbic acid under the following conditions: temperature of 70 °C, time of 4 h, and an L:S ratio of 10 cm<sup>3</sup>·g<sup>-1</sup>, resulted in a vanadium leaching yield of 98 wt.%. According to the authors, ascorbic acid enhances the dissolution of V<sub>2</sub>O<sub>5</sub> in the acid via an electron transfer mechanism, continuously converting VO<sub>2</sub><sup>+</sup> to V<sup>3+</sup> [116]. Alternatively, leaching with a hydrogen peroxide solution yielded a vanadium extraction efficiency of 92.2%. The SO<sub>2</sub> and H<sub>2</sub>SO<sub>4</sub> contained in the catalyst are oxidised by H<sub>2</sub>O<sub>2</sub>, thereby generating sulphuric acid in situ, which acts as the leaching agent. The determined optimal leaching conditions were an H<sub>2</sub>O<sub>2</sub> concentration of 148 g·dm<sup>-3</sup>, a very short leaching time of 5 min, a temperature of 25 °C, an agitation speed of 300 rpm, a catalyst particle size of <0.15 mm, and an L:S ratio of 3:1 [93]. Approximately 99 wt.% of vanadium extraction was achieved in a reductive leaching process conducted at 50 °C for 2 h, with an SO<sub>2</sub> to V molar ratio of 1.5 and a particle size smaller than 0.1 mm [117].

### 6.1.2. Caustic Leaching

A comparative analysis of hydrometallurgical processes shows that the choice of leaching medium is a critical factor determining the speciation and concentration of impurities in the pregnant leach solution (PLS), as well as influencing the selection of subsequent solution purification stages. Against this background, alkaline leaching processes, which offer a different mechanism for vanadium dissolution (Equations (14) and (15)), are of significant importance and constitute the subject of the next section. In contrast to acidic systems, alkaline leaching utilising NaOH, KOH, Na<sub>2</sub>CO<sub>3</sub>, or urea allows for the generation of solutions with significantly higher chemical purity.



During alkaline leaching of spent vanadium catalysts, partial dissolution of the silica-based support may occur (Equations (16) and (17)), resulting in the transfer of silicon species into the leachate in the form of soluble silicates, particularly at elevated OH<sup>-</sup> concentrations and increased process temperatures [118–120].



Despite a vanadium dissolution efficiency comparable to that observed in acidic solutions (ranging from 85% to 95%), the co-extraction of iron remains at a trace level (<2%), which is governed by the low solubility product of iron(III) hydroxides under high pH conditions. Consequently, the V/(Fe + Al) ratio in the alkaline PLS is an order of magnitude

higher (often exceeding 50), which reduces the number of required separation steps and enables the direct precipitation of polyprotonated vanadates [118–120]. Table 4 summarises selected literature reporting the alkaline leaching of vanadium oxide-containing catalysts.

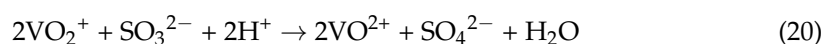
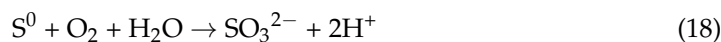
**Table 4.** Alkaline leaching systems for vanadium recovery from spent catalysts.

Alkaline Leaching System	Conditions (C, T, Time, L/S, Particle Size)	V Recovery from PLS (%)	Reference
NaOH	4 mol·dm <sup>-3</sup> , 100 °C, 5 h, 5 cm <sup>3</sup> ·g <sup>-1</sup> , particle size 0.105 mm	~99	[121]
NaOH + H <sub>2</sub> O <sub>2</sub>	5 wt.% NaOH, 30 wt.% H <sub>2</sub> O <sub>2</sub> , 25 °C, 1 h, 10 cm <sup>3</sup> ·g <sup>-1</sup> , particle size < 0.2 mm, L(H <sub>2</sub> O <sub>2</sub> )/S = 0.175 cm <sup>3</sup> ·g <sup>-1</sup>	91	[90]
(NH <sub>4</sub> ) <sub>2</sub> CO <sub>3</sub> + H <sub>2</sub> O <sub>2</sub>	10 wt.% (NH <sub>4</sub> ) <sub>2</sub> CO <sub>3</sub> , 30 wt.% H <sub>2</sub> O <sub>2</sub> , room temperature, 1 h, 10 cm <sup>3</sup> ·g <sup>-1</sup> , particle size n.d., L(H <sub>2</sub> O <sub>2</sub> )/S = 0.16 cm <sup>3</sup> ·g <sup>-1</sup>	94	[90]
KOH	15 wt.%, 50 °C, 4 h, 10 cm <sup>3</sup> ·g <sup>-1</sup> , particle size < 0.075 mm	86	[122]
Urea	40 wt.%, 20 °C, 1 h, 10 cm <sup>3</sup> ·g <sup>-1</sup> , particle size 0.18–0.25 mm	79	[123]

Roasting the catalyst at 400 °C followed by leaching the comminuted feedstock (particle size approx. 0.1 mm) with a 4 mol·dm<sup>-3</sup> NaOH solution at 80 °C for 2 h (at an L/S ratio of 10 cm<sup>3</sup>·g<sup>-1</sup>) resulted in a vanadium extraction efficiency of 78 wt.% [124].

### 6.1.3. Bioleaching

Biohydrometallurgy of secondary vanadium sources represents a promising alternative to conventional acid or alkaline leaching, allowing for a reduction in gaseous emissions and the generation of hazardous waste [125,126]. In this process, acidophilic, chemoautotrophic sulphur-oxidising bacteria of the genus *Acidithiobacillus*, such as *A. ferrooxidans* [127] and *A. thiooxidans* [128], play a crucial role. The selection of these microorganisms is dictated by the fact that vanadium possesses stable soluble forms in acidic environments (pH < 2.0) at high oxidation-reduction potentials (Eh > 500 mV) [129]. During the biooxidation of elemental sulphur, these bacteria produce intermediate species, such as sulphites (Equation (18)) and thiosulphates (Equation (19)), which exhibit strong reducing properties (Figure 9) [130], enabling the effective reduction of V(V) to V(IV) (Equation (20)) and enhancing extraction efficiency.



The efficiency of bioleaching processes is strongly influenced by operational conditions, particularly temperature, due to the temperature sensitivity of the microorganisms involved. Lower operating temperatures may reduce the activity of iron- and sulphur-oxidising microorganisms, resulting in slower leaching kinetics and longer processing times. Consequently, the application of bioleaching technologies in cold climatic regions may require additional process control measures to maintain satisfactory recovery efficiency and process stability [125–128].

In contrast, an alternative approach utilises heterotrophic leaching, where V-containing waste is processed using organic acids such as citric, gluconic, and oxalic acids which are metabolites produced by the fungus *Aspergillus niger* (Equation (21)) [131].

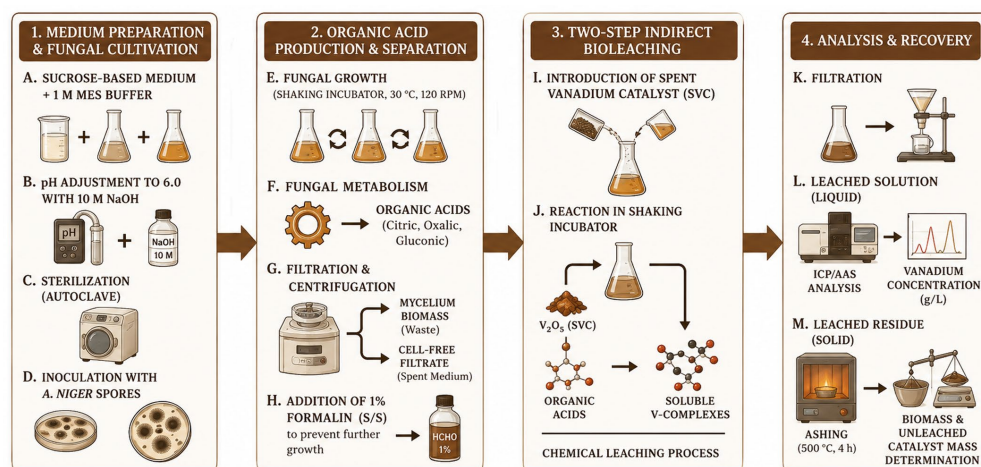
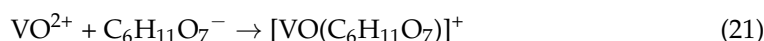


**Figure 9.** Proposed vanadium bioleaching scheme for SVC, based on the methodology described in [130].

## 6.2. Vanadium Separation Techniques from Pregnant Leach Solutions

Selective vanadium recovery from complex pregnant leach solutions (containing species such as Fe, Al, K, Si, and residual lixivants) necessitates process optimisation based on chemical speciation, solution pH, and the presence of competing ions [132,133]. The predominant separation techniques employed to achieve high product purity include adsorption, ion exchange (IX), solvent extraction (SX), and chemical precipitation.

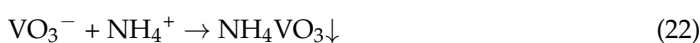
### 6.2.1. Adsorption with Activated Carbon

Adsorption onto activated carbon (AC) is a highly efficient method for vanadium removal, particularly suitable for treating solutions with low initial concentrations. The adsorption mechanism is driven by surface complexation, where surface hydroxyl groups are substituted by anionic vanadium species. Subsequent metal recovery and adsorbent regeneration are achieved through elution in alkaline media [62]. Conversely, highly acidic conditions inhibit the adsorption process due to a shift in vanadium speciation toward cationic forms, which exhibit negligible affinity for the AC surface active sites [134].

### 6.2.2. Precipitation

Chemical precipitation is one of the most widely used methods for recovering vanadium from leach solutions. The process is typically based on the addition of ammonium salts ( $\text{NH}_4\text{Cl}$ ,  $(\text{NH}_4)_2\text{SO}_4$ ,  $\text{NH}_4\text{NO}_3$ ,  $\text{CH}_3\text{COONH}_4$ ) (Equation (22)), leading to the selective precipitation of vanadium as ammonium metavanadate ( $\text{NH}_4\text{VO}_3$ ). As reported in the literature, the efficiency of vanadium recovery strongly depends on the type and concentration of the ammonium salt used, with precipitation yields often exceeding 98% [135].

In industrial practice,  $\text{NH}_4\text{Cl}$  is most commonly applied due to its economic advantages. However, its use in excess is necessary, as it enhances  $\text{NH}_4\text{VO}_3$  formation and reduces its solubility due to the common ion effect [124].



In a typical process, the suspension obtained after leaching is vacuum-filtered to separate Filtrate I, which is then subjected to a two-stage ammonification. In the first stage, a 25% ammonia solution is added at 80–90 °C until a pH of 6.0 is reached. Subsequently, the

resulting intermediate precipitate is treated with a 2% ammonia solution ( $12\text{--}16\text{ g}\cdot\text{dm}^{-3}$ ) and  $100\text{ g}\cdot\text{dm}^{-3}$   $\text{NH}_4\text{NO}_3$ . After separating Filtrate III, the resulting ammonium metavanadate ( $\text{NH}_4\text{VO}_3$ ) was dried at  $200\text{ }^\circ\text{C}$  and calcined at  $550\text{--}600\text{ }^\circ\text{C}$  (Equation (23)) for 3 h, yielding a final  $\text{V}_2\text{O}_5$  product with 98.2% purity. This process ensures a 97–98% recovery of the target material, effectively transforming the vanadium-containing solution into high-purity vanadium pentoxide (Figure 10) [136]. The process illustrated in Figure 11 ensures the recovery of vanadium(V) oxide with a purity of 98.5%. The procedure involves neutralising the solution obtained from the alkaline leaching of spent vanadium catalyst (SVC) with NaOH, followed by the reduction of V(V) to V(IV) using gaseous  $\text{SO}_2$ . Subsequently, hydrated vanadium(IV) oxide ( $\text{V}_2\text{O}_4\cdot x\text{H}_2\text{O}$ ) is precipitated using either gaseous ammonia or an ammonia solution [137].

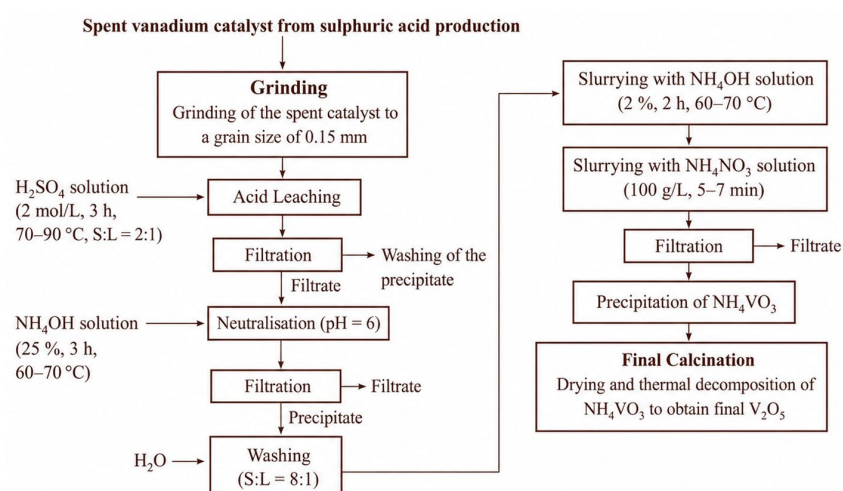
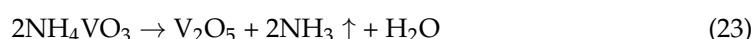


**Figure 10.** Flowsheet for the recovery of  $\text{V}_2\text{O}_5$  from spent vanadium catalyst used in sulphuric acid production through acid leaching and precipitation (based on [136]).

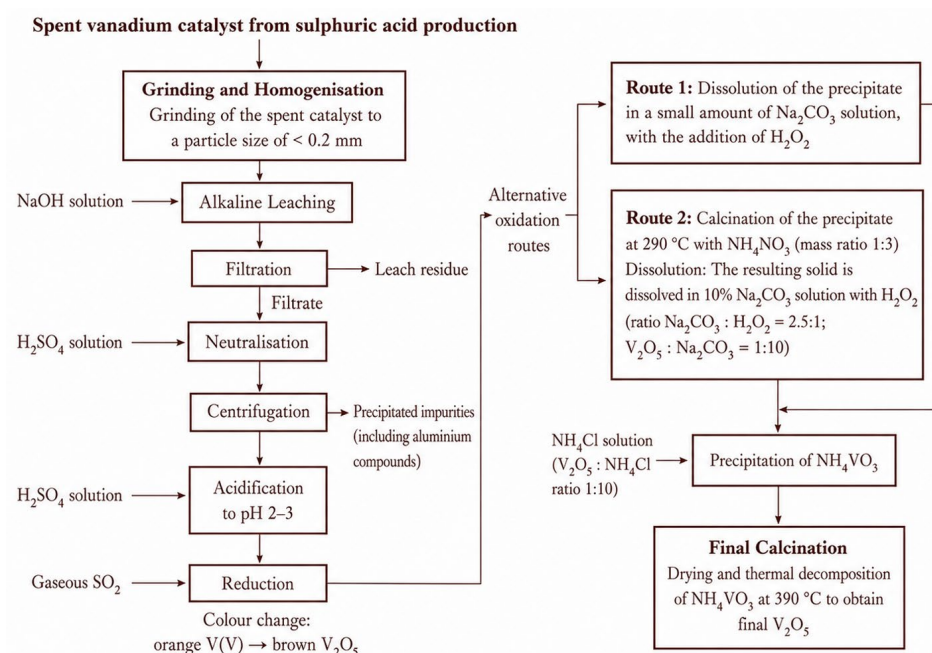


**Figure 11.** Flowsheet for the recovery of  $\text{V}_2\text{O}_5$  from spent vanadium catalyst used in sulphuric acid production through alkaline leaching and precipitation (based on [137]).

### 6.2.3. Solvent Extraction

Solvent extraction is a key step in the recovery of vanadium from leach solutions obtained from deactivated vanadium catalyst masses. In acidic sulphate leachates, vanadium is mainly present as V(IV) and V(V) species, and their separation and purification is carried out using different classes of extractants depending on the oxidation state of vanadium.

For V(IV) extraction, organophosphorus extractants such as di-(2-ethylhexyl)phosphoric acid (D2EHPA) [138], mono-2-ethylhexyl ester of 2-ethylhexylphosphonic acid (EHEHPA), and Cyanex 272 [139] are most commonly used. D2EHPA exhibits higher affinity for V(IV) than for V(V), and its distribution coefficients for V(IV) are sufficiently high for industrial application. The selectivity of extraction is strongly influenced by the presence of competing ions, following the order  $\text{Fe}^{3+} > \text{VO}_2^+ > \text{V}^{4+} > \text{Ca}^{2+} > \text{Mg}^{2+} > \text{Fe}^{2+} > \text{K}^+, \text{Na}^+$ , indicating co-extraction of Fe(III) with vanadium, while Fe(II) is not extracted. Therefore, selective vanadium recovery requires prior reduction of Fe(III) to Fe(II) to minimise iron co-extraction [140].

For purification and enrichment of V(V), amine-based extractants such as N1923 [141] or Aliquat 336 [142] are applied. These systems typically require adjustment of the solution pH to a narrow range of 1.5–2.0 to ensure efficient extraction, whereas the initial pH of acidic vanadium-bearing leachates is around 0.5, which necessitates preliminary neutralisation before extraction [141,142].

The extraction mechanism involving D2EHPA can be described by equilibrium reactions of metal-extractant complex formation (Equation (24)). In industrial practice, the concentration of D2EHPA is maintained at 0.2–0.4 M, with an operating pH of approximately 2. Prior to extraction, reducing agents such as  $\text{Na}_2\text{S}$  or  $\text{NaHS}$  are used to adjust the chemical form of vanadium. Stripping of the loaded organic phase is carried out using dilute sulphuric acid, enabling transfer of vanadium back into the aqueous phase for further recovery [139,140].



Following the sulphuric acid leaching of SVC, vanadium was recovered via solvent extraction using primary amines in kerosene, achieving a 99% recovery rate. The vanadium was subsequently precipitated as ammonium metavanadate, which was then dried and calcined to yield high-purity  $\text{V}_2\text{O}_5$  (98.2%). This sequence ensures the efficient transformation of the extracted metal into its stable oxide form [111].

### 6.2.4. Ion Exchange

The efficiency of vanadium recovery from solutions obtained after alkaline and acidic leaching of spent vanadium catalyst (SVC) is directly dependent on chemical speciation, which is determined by the pH and redox potential of the system. The selective separation of vanadium from iron and potassium impurities was evaluated using strong acid cation-exchange resins, including Amberlite IR-120 Plus (Santa Cruz Biotechnology, Dallas, TX, USA), Dowex 50W X4 (Thermo Fisher Scientific, Waltham, MA, USA), and Dowex 50W X4-100, after leaching spent vanadium catalyst (SVC) in sulphuric and oxalic acid media. In sulphuric acid solutions, the affinity sequence was observed as  $(\text{Fe}^{3+}/\text{Fe}^{2+}) < \text{K}^+ \ll (\text{VO}^{2+}/\text{VO}_2^+)$ . Dowex 50W X4 achieved a breakthrough volume of  $67 \text{ cm}^3$  (1.65 BV), enabling complete removal of Fe and 99.96% removal of K, while adsorbing 39.5% of vanadium.

Leaching with oxalic acid significantly improved separation efficiency, particularly for Dowex 50W X4-100, which adsorbed 91% of Fe and 94% of K with only approximately 2% vanadium loss for a  $100 \text{ cm}^3$  sample volume. In contrast, Amberlite IR-120 Plus exhibited the lowest selectivity, with vanadium adsorption reaching 29%, indicating that oxalic acid provides a more favourable medium for vanadium purification. Furthermore, increasing

the resin grain size reduced vanadium affinity, facilitating optimisation of the process mass balance for high-purity  $V_2O_5$  recovery [74,143].

The kinetics of vanadium ion exchange on SBA anion exchangers (e.g., Purolite A400 (Purolite LCC, King of Prussia, PA, USA) and chelating resins (Lewatit AF5 (LANXES, Cologne, Germany)) are best described by the pseudo-second-order (PSO) kinetic model, indicating that chemisorption is the rate-limiting step of the process. Studies conducted using real SVC leach solutions showed correlation coefficients of  $R^2 > 0.99$  for the PSO model, with rate constants ( $k_2$ ) on the order of  $10^{-3}$ – $10^{-4}$   $g \cdot mg^{-1} \cdot min^{-1}$ . It was further reported that sorption capacities in real systems can reach up to  $248 mg \cdot g^{-1}$  for specialised resins (e.g., Dowex M4195), significantly exceeding the capacities obtained with conventional ion exchangers [144].

### 6.3. Management of Silica Residue and Secondary Waste Generated After Vanadium Recovery

After completion of the vanadium recovery process, two principal waste streams are generated: a silica-rich solid residue and secondary process waste, including post-leaching liquors and precipitated metal-containing sludge.

The silica residue obtained after alkaline leaching may be reused as a secondary raw material for the preparation of fresh vanadium catalysts, provided that its chemical composition and porous structure meet the technological requirements for catalyst production. The results of Grzesiak et al. confirmed that silica recovered from spent catalysts can be successfully use as a catalyst carrier. Alternatively, purified silica residue may be utilised as a mineral additive in the cement or construction materials industry, where silica-containing secondary materials are commonly applied [80,145–147].

In contrast, residues containing elevated concentrations of vanadium, iron, copper, potassium or other heavy metals require further stabilisation prior to disposal. Such waste may be treated by solidification/stabilisation using cementing agents together with calcium polysulphide and alkaline additives. This treatment reduces the mobility and leachability of vanadium and heavy metals through the formation of poorly soluble compounds. The stabilised material may subsequently be used as underground mine backfill or deposited in controlled hazardous waste landfills in accordance with environmental regulations [80,145–147].

## 7. Conclusions

The production volume of sulphuric acid is considered one of the key parameters that determine the development of a country's chemical industry. Therefore, vanadium compounds, particularly vanadium(V) oxide, play a crucial role. Vanadium pentoxide is traditionally used as a catalyst in the production of sulphuric acid and in the metallurgy, glass, and ceramics industries. During the first decade of the XXI century, this compound gained strategic raw material status thanks to its use in vanadium redox flow battery (VRFB) cells, which enable the construction of efficient energy storage systems for power grids. The growing range of applications for vanadium compounds, combined with the limited availability of natural resources and environmental concerns, creates a need to recover these compounds from waste.

As detailed in the article, the greatest challenge in using vanadium catalysts to produce sulphuric acid is their gradual deactivation. The processes that damage the catalysts are multifaceted and include thermal degradation, chemical poisoning, and mechanical damage. Excessive temperatures lead to the sintering of the active phase support and phase transformations of the silica, resulting in a reduction in the active surface area. The presence of chemical contaminants in the process gas, such as arsenic, fluorine, chlorine, or iron, can lead to the formation of stable, inactive chemical complexes that damage the porous

structure of the support. These phenomena reduce the catalytic activity and efficiency of the entire technological process, necessitating the replacement of the catalytic material. Spent catalysts become environmentally harmful industrial waste.

The need to manage spent contact mass has driven the development of technologies for recovering vanadium compounds, particularly hydrometallurgical processes such as acid and alkaline leaching. Under optimal conditions, these methods can achieve vanadium leaching efficiencies of approximately 95%, depending on the composition and degree of deactivation of the spent catalyst material. Following the leaching stage, additional purification procedures, including solvent extraction, precipitation, ion exchange, and calcination, are commonly applied to obtain vanadium products of sufficiently high quality for industrial reuse. The studies discussed in this review demonstrate that these integrated recovery approaches can produce high-purity  $V_2O_5$ , typically in the range of approximately 98–99%. The final purity of the recovered vanadium oxide is strongly influenced by the effectiveness of impurity removal during purification stages, as well as by the chemical composition of the initial spent catalyst. Residual impurities may include alkali metals, iron, aluminium, silicon, and sulphur-containing compounds, the concentrations of which depend on both process conditions and catalyst history.

Despite the significant progress achieved in vanadium recovery technologies, the economic aspects of these processes remain insufficiently addressed in the available literature. In particular, there is still limited information regarding the overall operational costs associated with catalyst processing, reagent consumption, waste neutralisation, energy demand, and downstream purification stages. Moreover, direct comparisons between the costs of secondary vanadium recovery and the market value of primary  $V_2O_5$  are rarely reported. Consequently, further research should focus not only on improving recovery efficiency and product purity, but also on comprehensive techno-economic assessments of vanadium recovery technologies to better evaluate their industrial feasibility and environmental sustainability.

It is also noteworthy that environmentally friendly solutions, such as bioleaching and the use of eutectic solvents, are becoming increasingly important. The sustainable management of vanadium compounds in sulphuric acid production requires a multifaceted approach. Alongside managing and disposing of used catalysts, it is also crucial to develop a new generation of catalysts that are less susceptible to chemical poisoning and more chemically resistant. Research into new catalysts involves using modern promoters such as cesium and cerium, optimising carrier shapes, and employing artificial intelligence to design materials and monitor their condition during plant operation. Concurrently, research is being conducted on the management and utilisation of by-products from the vanadium compound recovery process. For instance, silica residues can be used in construction and in producing mineral fertilisers. Taking a multifaceted approach to the effective management of vanadium catalysts presents a significant technological challenge and is an important part of ensuring the security of raw materials and the sustainable development of the chemical industry.

**Author Contributions:** Conceptualization, K.M.; investigation, S.D., A.W.-K. and K.M.; writing-original draft preparation, S.D., A.W.-K. and K.M.; writing-review and editing, S.D., B.I., K.M. and U.K.; visualization, S.D., A.W.-K., K.M. and U.K. All authors have read and agreed to the published version of the manuscript.

**Funding:** This research received no external funding.

**Data Availability Statement:** No new data were created or analyzed in this study. Data sharing is not applicable to this article.

**Acknowledgments:** During the preparation of this manuscript/study, the authors used Google Gemini 3 and ChatGPT (GPT 5.5) for the purposes of generating Figures 3, 5, 6 and 9, and the graphical abstract. The authors have reviewed and edited the output and take full responsibility for the content of this publication.

**Conflicts of Interest:** The authors declare no conflicts of interest.

## References

1. European Commission. JRC RMIS. Critical and Strategic Materials. 2024. Available online: <https://rmis.jrc.ec.europa.eu/critical-and-strategic-materials> (accessed on 9 April 2026).
2. U.S. Geological Survey. Vanadium. In *2023 Minerals Yearbook*; U.S. Geological Survey: Reston, VA, USA, 2026. Available online: <https://pubs.usgs.gov/periodicals/mcs2023/mcs2023.pdf> (accessed on 12 April 2026).
3. Rogers, B.L.; Banerjee, S. Mine the Gap: Sourcing Vanadium for the Energy Transition. *Joule* **2025**, *9*, 102139. [[CrossRef](#)]
4. Temam, A.G.; Alshoabi, A.; Getaneh, S.A.; Awada, C.; Nwanya, A.C.; Ejikeme, P.M.; Ezema, F.I. Recent Progress on V<sub>2</sub>O<sub>5</sub> Based Electroactive Materials: Synthesis, Properties, and Supercapacitor Application. *Curr. Opin. Electrochem.* **2023**, *38*, 101239. [[CrossRef](#)]
5. Le, T.K.; Pham, P.V.; Dong, C.; Bahlawane, N.; Vernardou, D.; Mjejri, I.; Rougier, A.; Kim, S.W. Recent advances in vanadium pentoxide (V<sub>2</sub>O<sub>5</sub>) towards related applications in chromogenics and beyond: Fundamentals, progress, and perspectives. *J. Mater. Chem. C* **2022**, *10*, 4019–4071. [[CrossRef](#)]
6. Karapidakis, E.; Vernardou, D. Progress on V<sub>2</sub>O<sub>5</sub> Cathodes for Multivalent Aqueous Batteries. *Materials* **2021**, *14*, 2310. [[CrossRef](#)] [[PubMed](#)]
7. Li, Y.; Chen, S.; Duan, W.; Nan, Y.; Ding, D.; Xiao, G. Research Progress of Vanadium Pentoxide Photocatalytic Materials. *RSC Adv.* **2023**, *13*, 22945–22957. [[CrossRef](#)]
8. Hu, P.; Hu, P.; Vu, T.D.; Li, M.; Wang, S.; Ke, Y.; Zeng, X.; Mai, L.; Long, Y. Vanadium Oxide: Phase Diagrams, Structures, Synthesis, and Applications. *Chem. Rev.* **2023**, *123*, 4353–4415. [[CrossRef](#)]
9. Gamal, H.; Elshahawy, A.M.; Medany, S.S.; Hefnawy, M.A.; Shalaby, M.S. Recent Advances of Vanadium Oxides and Their Derivatives in Supercapacitor Applications: A Comprehensive Review. *J. Energy Storage* **2024**, *76*, 109788. [[CrossRef](#)]
10. Kiran, P.; Jasrotia, P.; Verma, A.; Kumar, A.; Hmar, J.J.L.; Jyoti; Kumar, T. Vanadium Pentoxide Gas Sensors: An Overview of Elemental Doping Strategies and Their Effect on Sensing Performance. *Catal. Commun.* **2024**, *187*, 106838. [[CrossRef](#)]
11. Tolstopyatova, E.G.; Salnikova, Y.D.; Holze, R.; Kondratiev, V.V. Progress and Challenges of Vanadium Oxide Cathodes for Rechargeable Magnesium Batteries. *Molecules* **2024**, *29*, 3349. [[CrossRef](#)]
12. Li, H.; Wu, J.; Li, M.; Wang, Y. Recent Advances in Vanadium-Based Electrocatalysts for Hydrogen and Oxygen Evolution Reactions: A Review. *Catalysts* **2024**, *14*, 368. [[CrossRef](#)]
13. Mazidi, M.; Mosayebi Behbahani, R.; Fazeli, A. Ce Promoted V<sub>2</sub>O<sub>5</sub> Catalyst in Oxidation of SO<sub>2</sub> Reaction. *Appl. Catal. B-Environ.* **2017**, *209*, 190–202. [[CrossRef](#)]
14. Vo, P.N.X.; Nguyen, L.-P.; Tran, T.V.; Ngo, P.T.; Luong, T.N. Oxidative Regeneration Study of Spent V<sub>2</sub>O<sub>5</sub> Catalyst from Sulfuric Acid Manufacture. *React. Kinet. Mech. Catal.* **2018**, *125*, 887–900. [[CrossRef](#)]
15. Grobela, M.; Grzesiak, P. The Influence of Iron Compounds in the Sulfuric Acid Catalyst on the SO<sub>2</sub> Oxidation Process. *Pol. J. Chem. Technol.* **2007**, *9*, 2–6. [[CrossRef](#)]
16. Balzhinimaev, B.S.; Ivanov, A.A.; Lapina, O.B.; Mastikhin, V.M.; Zamaraev, K.I. Mechanism of Sulphur Dioxide Oxidation over Supported Vanadium Catalysts. *Faraday Discuss. Chem. Soc.* **1989**, *87*, 133–147. [[CrossRef](#)]
17. Zhang, W.; Qi, S.; Pantaleo, G.; Liotta, L.F. WO<sub>3</sub>-V<sub>2</sub>O<sub>5</sub> Active Oxides for NO<sub>x</sub> SCR by NH<sub>3</sub>: Preparation Methods, Catalysts' Composition, and Deactivation Mechanism—A Review. *Catalysts* **2019**, *9*, 527. [[CrossRef](#)]
18. Busca, G.; Lietti, L.; Ramis, G.; Berti, F. Chemical and Mechanistic Aspects of the Selective Catalytic Reduction of NO<sub>x</sub> by Ammonia over Oxide Catalysts: A Review. *Appl. Catal. B-Environ.* **1998**, *18*, 1–36. [[CrossRef](#)]
19. Zhao, S.; Peng, J.; Ge, R.; Yang, K.; Wu, S.; Qian, Y.; Xu, T.; Gao, J.; Chen, Y.; Sun, Z. Poisoning and Regeneration of Commercial V<sub>2</sub>O<sub>5</sub>-WO<sub>3</sub>/TiO<sub>2</sub> Selective Catalytic Reduction (SCR) Catalyst in Coal-Fired Power Plants. *Process Saf. Environ. Prot.* **2022**, *168*, 971–992. [[CrossRef](#)]
20. Rajath, S.; Bagewadi, M.; Shivakumar, N.D. V<sub>2</sub>O<sub>5</sub>-TiO<sub>2</sub> SCR Plate Catalysts for High Dust De-NO<sub>x</sub> Applications: A Comprehensive Characterization Study. *Emiss. Control Sci. Technol.* **2025**, *11*, 25. [[CrossRef](#)]
21. Gnanasekaran, L.; Rajendran, S.; Karimi-Maleh, H.; Priya, A.K.; Qin, J.; Soto-Moscoso, M.; Ansar, S.; Bathula, C. Surface Modification of TiO<sub>2</sub> by Adding V<sub>2</sub>O<sub>5</sub> Nanocatalytic System for Hydrogen Generation. *Chem. Eng. Res. Des.* **2022**, *182*, 114–119. [[CrossRef](#)]
22. Vinodh, R.; Pollet, B.G. Facile and cost-effective nickel-anchored nanofibril V<sub>2</sub>O<sub>5</sub> electrocatalyst for efficient oxygen evolution reaction. *Int. J. Hydrogen Energy* **2025**, *113*, 395–405. [[CrossRef](#)]

23. Nandana, A.B.; Anand, A.C.; George, S.M.; Rakhi, R.B. Electrochemical Investigation of  $V_2O_5$  as a High-Performance Material for Supercapacitors and Electrocatalysis. *ACS Appl. Electron. Mater.* **2026**, *8*, 634–644. [CrossRef]
24. Schneider, K.; Lubecka, M.; Czaplá, A.  $V_2O_5$  Thin Films for Gas Sensor Applications. *Sens. Actuators B Chem.* **2016**, *236*, 970–977. [CrossRef]
25. Majumdar, D.; Mandal, M.; Bhattacharya, S.K.  $V_2O_5$  and Its Carbon-Based Nanocomposites for Supercapacitor Applications. *ChemElectroChem* **2019**, *6*, 1623–1648. [CrossRef]
26. Zhang, W.; Zuo, C.; Tang, C.; Tang, W.; Lan, B.; Fu, X.; Dong, S.; Luo, P. The Current Developments and Perspectives of  $V_2O_5$  as Cathode for Rechargeable Aqueous Zinc-Ion Batteries. *Energy Technol.* **2021**, *9*, 2000789. [CrossRef]
27. Li, Y.; Huang, Z.; Kalambate, P.K.; Zhong, Y.; Huang, Z.; Xie, M.; Shen, Y.; Huang, Y.  $V_2O_5$  Nanopaper as a Cathode Material with High Capacity and Long Cycle Life for Rechargeable Aqueous Zinc-Ion Battery. *Nano Energy* **2019**, *60*, 752–759. [CrossRef]
28. Babar, B.M.; Sutar, S.H.; Mujawar, S.H.; Patil, S.S.; Babar, U.D.; Pawar, U.T.; Kadam, P.M.; Patil, P.S.; Kadam, L.D.  $V_2O_5$ -rGO Based Chemiresistive Gas Sensor for  $NO_2$  Detection. *Mater. Sci. Eng. B* **2023**, *298*, 116827. [CrossRef]
29. Zhang, F.; Qu, Y.; Lu, X.; Ding, Z.; Li, S.; Ji, W.; Liu, S. Double-Shelled Hollow Sphere  $V_2O_5$ -Based Conductometric Ethanol Gas Sensor. *Sens. Actuators B Chem.* **2024**, *417*, 136009. [CrossRef]
30. Wang, Z.; Liu, Y.; Zhang, Y.; Dong, Y.; Jiang, Z.; Zhang, L.; Liu, W.; Guan, J.; Lin, H. Efficient and Sustainable Photocatalytic Degradation of Dye in Wastewater with Porous and Recyclable Wood Foam@ $V_2O_5$  Photocatalysts. *J. Clean. Prod.* **2022**, *332*, 130054. [CrossRef]
31. Shalini, K.S.; Kavitha, R.; Basavarajaiah, S.M.; Nirmala, B. Green Synthesis of  $\alpha$ - $V_2O_5$  Photocatalyst Using *Gymnema sylvestre* Leaf Extract and an Insight into the Mechanism of Photocatalytic Degradation of Methylene Blue and Congo Red under Visible Light Illumination. *Next Sustain.* **2026**, *7*, 100267. [CrossRef]
32. Yadav, A.A.; Hunge, Y.M.; Kang, S.-W.; Fujishima, A.; Terashima, C. Enhanced Photocatalytic Degradation Activity Using the  $V_2O_5$ /rGO Composite. *Nanomaterials* **2023**, *13*, 338. [CrossRef]
33. Mahnoor, M.; Chandio, R.; Inam, A.; Ahad, I.U. Critical and Strategic Raw Materials for Energy Storage Devices. *Batteries* **2025**, *11*, 163. [CrossRef]
34. Simandl, G.J.; Paradis, S. Vanadium as a Critical Material: Economic Geology with Emphasis on Market and the Main Deposit Types. *Appl. Earth Sci.* **2022**, *131*, 218–236. [CrossRef]
35. U.S. Geological Survey. *Mineral Commodity Summaries 2026*; U.S. Geological Survey: Reston, VA, USA, 2026. [CrossRef]
36. U.S. Geological Survey. Vanadium. In *Minerals Yearbook 2022: Metals and Minerals*; U.S. Geological Survey: Reston, VA, USA, 2026. Available online: <https://pubs.usgs.gov/myb/vol1/2022/myb1-2022-vanadium.pdf> (accessed on 12 April 2026).
37. U.S. Geological Survey. Vanadium. In *Minerals Yearbook 2018: Metals and Minerals*; U.S. Geological Survey: Reston, VA, USA, 2021. Available online: <https://d9-wret.s3.us-west-2.amazonaws.com/assets/palladium/production/atoms/files/myb1-2018-vanad.pdf> (accessed on 12 April 2026).
38. U.S. Geological Survey. Vanadium. In *Minerals Yearbook 2010: Metals and Minerals*; U.S. Geological Survey: Reston, VA, USA, 2012. Available online: <https://d9-wret.s3.us-west-2.amazonaws.com/assets/palladium/production/mineral-pubs/vanadium/myb1-2010-vanad.pdf> (accessed on 12 April 2026).
39. U.S. Geological Survey. Vanadium. In *Minerals Yearbook 2005: Metals and Minerals*; U.S. Geological Survey: Reston, VA, USA, 2007. Available online: <https://d9-wret.s3.us-west-2.amazonaws.com/assets/palladium/production/mineral-pubs/vanadium/vanadmyb05.pdf> (accessed on 12 April 2026).
40. U.S. Geological Survey. Vanadium. In *Minerals Yearbook 2001: Metals and Minerals*; U.S. Geological Survey: Reston, VA, USA, 2003. Available online: <https://d9-wret.s3.us-west-2.amazonaws.com/assets/palladium/production/mineral-pubs/vanadium/vanamyb01.pdf> (accessed on 12 April 2026).
41. Hossain, M.H.; Abdullah, N.; Tan, K.H.; Saidur, R.; Mohd Radzi, M.A.; Shafie, S. Evolution of Vanadium Redox Flow Battery in Electrode. *Chem. Rec.* **2024**, *24*, e202300092. [CrossRef]
42. Puleston, T.; Clemente, A.; Costa-Castelló, R.; Serra, M. Modelling and Estimation of Vanadium Redox Flow Batteries: A Review. *Batteries* **2022**, *8*, 121. [CrossRef]
43. Al Amayreh, H.H.; Al-Harabsheh, M.; Al-Otoom, A.Y.; Al-Makhadmeh, L.; Al-Harabsheh, A.M. The Recovery of Vanadium Pentoxide ( $V_2O_5$ ) from Spent Catalyst Utilized in a Sulfuric Acid Production Plant in Jordan. *Materials* **2023**, *16*, 6503. [CrossRef]
44. Romanovskaia, E.; Romanovski, V.; Kwapinski, W.; Kurilo, I. Selective Recovery of Vanadium Pentoxide from Spent Catalysts of Sulfuric Acid Production: Sustainable Approach. *Hydrometallurgy* **2021**, *200*, 105568. [CrossRef]
45. El Hasbaoui, N.; Elhadrami, A.; Brahmi, R. Method for Regenerating Spent Catalyst Used to Produce Sulfuric Acid in the  $SO_2$  to  $SO_3$  Conversion Step. *Mater. Sci. Forum* **2025**, *1173*, 113–121. [CrossRef]
46. Wagenfeld, J.-G.; Al-Ali, K.; Almheiri, S.; Slavens, A.F.; Calvet, N. Sustainable applications utilizing sulfur, a by-product from oil and gas industry: A state-of-the-art review. *Waste Manag.* **2019**, *95*, 78–89. [CrossRef]
47. Maslin, M.; Van Heerde, L.; Day, S. Sulfur: A potential resource crisis that could stifle green technology and threaten food security as the world decarbonises. *Geogr. J.* **2022**, *188*, 498–505. [CrossRef]

48. U.S. Geological Survey. *Mineral Commodity Summaries 2025*; U.S. Geological Survey: Reston, VA, USA, 2025. [CrossRef]
49. U.S. Geological Survey. *Mineral Commodity Summaries 2020*; U.S. Geological Survey: Reston, VA, USA, 2020. [CrossRef]
50. Bertau, M.; Wellmer, F.-W.; Scholz, R.W.; Mew, M.; Zenk, L.; Aubel, I.; Fröhlich, P.; Raddant, M.; Steiner, G. The Future of Phosphoric Acid Production—Why We Have to Leave Trodden Paths. *ChemSusChem* **2025**, *18*, e202401155. [CrossRef] [PubMed]
51. Davenport, W.G.; King, M.J.; Moats, M.S.; Schlesinger, M.E. *Sulfuric Acid Manufacture: Analysis, Control and Optimization*; Elsevier: Oxford, UK, 2013.
52. Sharma, R.K.; Cox, M.S.; Oglesby, C.; Dhillon, J.S. Revisiting the role of sulfur in crop production: A narrative review. *J. Agric. Food Res.* **2024**, *15*, 101013. [CrossRef]
53. Ciesielczyk, F.; Jesionowski, T. Inorganic Acids—Technology Background and Future Perspectives. *Phys. Sci. Rev.* **2020**, *5*, 20190030. [CrossRef]
54. Toledo, A.G.R.; Bevilaqua, D.; Panda, S.; Akcil, A. Hydrometallurgical processing of sulfide minerals from the perspective of semiconductor electrochemistry: A review. *Miner. Eng.* **2023**, *200*, 10x09. [CrossRef]
55. León, F.; Rojas, L.; Bazán, V.; Martínez, Y.; Peña, A.; Garcia, J. A systematic review of copper heap leaching: Key operational variables, green reagents, and sustainable engineering strategies. *Processes* **2025**, *13*, 1513. [CrossRef]
56. Zhao, K.; Gao, F.; Yang, Q. Comprehensive review on metallurgical upgradation processes of nickel sulfide ores. *J. Sustain. Metall.* **2022**, *8*, 1169–1195. [CrossRef]
57. Zhang, W.; Li, X.; Zhao, L.; Sun, W. Comparative Analysis of Sulfuric-Acid-Catalyzed Isobutane-Butene Alkylation Based on Kinetic Modeling. *Processes* **2025**, *13*, 1604. [CrossRef]
58. Ivashkina, E.N.; Ivanchina, E.D.; Nurmakanova, A.E.; Boychenko, S.S.; Ushakov, A.S.; Dolganova, I.O. Mathematical Modeling of Sulfuric Acid Catalyzed Alkylation of Isobutane with Olefins. *Procedia Eng.* **2016**, *152*, 81–86. [CrossRef]
59. Xin, Z.; Jiang, H.; Zhang, Z.; Chen, Y.; Wang, J. Kinetic Model of Olefins/Isobutane Alkylation Using Sulfuric Acid as Catalyst. *ACS Omega* **2022**, *7*, 9513–9526. [CrossRef] [PubMed]
60. Tian, S.; Wang, Y.; Zhang, X.; Li, J. Case Study for Enhancing Concentration of Waste Dilute Sulfuric Acid. *Sep. Purif. Technol.* **2023**, *312*, 123373. [CrossRef]
61. Li, W.; Erickson, E.M.; Manthiram, A. High-Nickel Layered Oxide Cathodes for Lithium-Based Automotive Batteries. *Nat. Energy* **2020**, *5*, 26–34. [CrossRef]
62. Li, H.; Xing, S.; Liu, Y.; Li, F.; Guo, H.; Kuang, G. Recovery of Lithium, Iron, and Phosphorus from Spent LiFePO<sub>4</sub> Batteries Using Stoichiometric Sulfuric Acid Leaching System. *ACS Sustain. Chem. Eng.* **2017**, *5*, 8017–8024. [CrossRef]
63. Ukwuani, A.T.; Tao, W. Developing a Vacuum Thermal Stripping-Acid Absorption Process for Ammonia Recovery from Digestate. *Water Res.* **2016**, *106*, 108–117. [CrossRef] [PubMed]
64. Shannak, S.; Cochrane, L.; Bobarykina, D. Strategic Analysis of Metal Dependency in the Transition to Low-Carbon Energy: A Critical Examination of Nickel, Cobalt, Lithium, Graphite, and Copper Scarcity. *Energy Res. Soc. Sci.* **2024**, *118*, 103773. [CrossRef]
65. Kiefer, D.M. Sulfuric acid: Pumping up the volume. *Today's Chem. Work* **2001**, *10*, 57–58.
66. Ashar, N.G.; Golwalkar, K.R. *A Practical Guide to the Manufacture of Sulfuric Acid, Oleums, and Sulfonating Agents*; Springer: Cham, Switzerland, 2013. [CrossRef]
67. d'Aquin, G.E.; Fell, R.C. Sulfur and Sulfuric Acid. In *Handbook of Industrial Chemistry and Biotechnology*, 12th ed.; Kent, J.A., Ed.; Springer: Boston, MA, USA, 2012. [CrossRef]
68. Grzesiak, P. Methods and Technologies of Sulphuric Acid Production. In *Sulphuric Acid*; Institute of Plant Protection (IOR): Poznań, Poland, 2002; Volume 1. (In Polish)
69. Müller, H. Sulfuric Acid and Sulfur Trioxide. In *Ullmann's Encyclopedia of Industrial Chemistry*; Wiley-VCH: Weinheim, Germany, 2000. [CrossRef]
70. European Commission. *Best Available Techniques (BAT) Reference Document for the Production of Large Volume Inorganic Chemicals—Ammonia, Acids and Fertilisers*; Publications Office of the European Union: Luxembourg, 2017.
71. Grzesiak, P. Best Available Techniques (BAT) in Sulphuric Acid Production. In *Sulphuric Acid*; Institute of Plant Protection (IOR): Poznań, Poland, 2004; Volume 2. (In Polish)
72. Vernikovskaya, N.V.; Zagoruiko, A.N.; Noskov, A.S. SO<sub>2</sub> oxidation method: Mathematical modeling taking into account dynamic properties of the process. *Chem. Eng. Sci.* **1999**, *54*, 5239–5246. [CrossRef]
73. Grzesiak, P. Vanadium Catalysts for the Oxidation of SO<sub>2</sub>. In *Sulphuric Acid*; Institute of Plant Protection (IOR): Poznań, Poland, 2005; Volume 5. (In Polish)
74. Mazurek, K. Recovery of vanadium, potassium and iron from a spent vanadium catalyst by oxalic acid solution leaching, precipitation and ion exchange processes. *Hydrometallurgy* **2013**, *134–135*, 26–31. [CrossRef]
75. Ksibi, M.; Elaloui, E.; Houas, A.; Moussa, N. Diagnosis of deactivation sources for vanadium catalysts used in SO<sub>2</sub> oxidation reaction and optimization of vanadium extraction from deactivated catalysts. *Appl. Surf. Sci.* **2003**, *220*, 105–112. [CrossRef]
76. Cavalca, F.; Beato, P.; Hyldtoft, J.; Christensen, K.; Helveg, S. Vanadia-based catalysts for the sulfur dioxide oxidation studied in situ by transmission electron microscopy and raman spectroscopy. *J. Phys. Chem. C* **2017**, *121*, 3350–3364. [CrossRef]

77. EL Hasbaoui, N.; EL Hadrami, A.; Brahmi, R. Accelerated deactivation of industrial SO<sub>2</sub> oxidation catalysts in sulfuric acid production. *Comptes Rendus Chim.* **2026**, *29*, 99–105. [CrossRef]
78. Li, X.; Yao, D.; Wu, F.; Wang, X.; Wei, L.; Liu, B. New findings in hydrothermal deactivation research on the vanadia-selective catalytic reduction catalyst. *ACS Omega* **2019**, *4*, 5088–5097. [CrossRef]
79. Li, J.; Zhang, P.; Chen, L.; Zhang, Y.; Qi, L. Regeneration of selective catalyst reduction catalysts deactivated by Pb, As, and alkali metals. *ACS Omega* **2020**, *5*, 13886–13893. [CrossRef]
80. Mikoda, B.; Potysz, A.; Gruszecka-Kosowska, A.; Kmieciak, E.; Tomczyk, A. Spent sulfuric acid plant catalyst: Valuable resource of vanadium or risky residue? Process comparison for environmental implications. *Environ. Sci. Pollut. Res.* **2021**, *28*, 59358–59367. [CrossRef] [PubMed]
81. European Sulphuric Acid Association & Fertilizers Europe. Best Available Techniques for Pollution Prevention and Control in the European Sulphuric Acid and Fertilizer Industries. In *Booklet No. 3 of 8*, 2nd ed.; ESA/Fertilizers Europe: Brussels, Belgium, 2000.
82. Perdomo Gómez, L.; Perdomo González, L.; Coello Machado, N.; Glistau, E. Vanadium recovery from spent catalyst: From lab to industry. *Int. J. Eng.* **2024**, *22*, 59–70.
83. Wang, X.; Kang, Y.; Li, J.; Li, D. Influence of cerium and cesium promoters on vanadium catalyst for sulfur dioxide oxidation. *Korean J. Chem. Eng.* **2019**, *36*, 650–659. [CrossRef]
84. Cheng, W.; Li, J.; Deng, J.; Li, Y.; Cheng, F. Leaching vanadium from the spent denitration catalyst in the sulfuric acid/oxalic acid combined solvent. *ACS Omega* **2024**, *9*, 9286–9294. [CrossRef]
85. Du, X.; Xue, J.; Wang, X.; Chen, Y.; Ran, J.; Zhang, L. Oxidation of sulfur dioxide over V<sub>2</sub>O<sub>5</sub>/TiO<sub>2</sub> catalyst with low vanadium loading: A theoretical study. *J. Phys. Chem. C* **2018**, *122*, 4517–4523. [CrossRef]
86. Chen, B.; Guo, Y.; Du, H.; Wang, S.; Liu, B.; Li, L. Review of Vanadium Production Part II: Secondary Resources. *Min. Metall. Explor.* **2026**, *43*, 769–791. [CrossRef]
87. Wen, J.; Wang, X.; Yu, F.; Tian, M.; Wang, C.; Huang, G.; Xu, S. Recovery and Value-Added Utilization of Critical Metals from Spent Catalysts for New Energy Industry. *J. Clean. Prod.* **2023**, *419*, 138295. [CrossRef]
88. Zeng, F.; Van Caneghem, J.; Granata, G. Alkaline Leaching of Spent SCR Catalysts: Mechanochemical Activation vs. Mechanochemical Leaching. *Sep. Purif. Technol.* **2026**, *390*, 136806. [CrossRef]
89. Yu, H.; Liu, S.; Yaraş, A.; Enkhchimeg, B.; Hu, L.; Zhang, W.; Peng, M.; Arslanoğlu, H.; Mao, L. Recovery of Valuable Metals from Spent Hydrodesulfurization (HDS) Catalysts: A Comprehensive Research Review and Specific Industrial Cases. *J. Environ. Manag.* **2025**, *379*, 124920. [CrossRef]
90. Trypuć, M.; Grzesiak, P.; Mazurek, K.; Grobela, M. *Kompleksowe Zagospodarowanie Szkodliwych Odpadów Katalizatora Wanadowego Stosowanego Do Utleniania SO<sub>2</sub>, Tom 1, Charakterystyka Procesów i Katalizatorów w Produkcji Kwasu Siarkowego [Comprehensive Management of Harmful Waste of Vanadium Catalyst Used for SO<sub>2</sub> Oxidation, Volume 1, Characteristics of Processes and Catalysts in Sulfuric Acid Production]*; Wydawnictwo Naukowe Instytutu Ochrony Roślin w Poznaniu: Poznań, Poland, 2007; p. 195. (In Polish)
91. Garcia, D.J.; Lozano Blanco, L.J.; Mulero Vivancos, M.D. Leaching of Vanadium from Sulphuric Acid Manufacture Spent Catalysts. *Rev. Metal. Madrit.* **2001**, *37*, 18–23. [CrossRef]
92. Perdomo Gómez, L.A.; Perdomo González, L.; Coello Machado, N.I.; Glistau, E. Processing Strategy for Catalytic Residues Containing Vanadium. In *Otto-Von-Guericke Universität Magdeburg*; OVGU: Magdeburg, Germany, 2024. [CrossRef]
93. Wu, L.; Dai, C.; Wang, H.; Wang, J.; Dong, Y. Leaching of Vanadium, Potassium, and Iron from Spent Catalyst of the Manufacture of Sulfuric Acid. *J. Mater. Res. Technol.* **2021**, *11*, 905–913. [CrossRef]
94. Shaltout, A.; El-Hallag, R.; Razek, T. Green Recovery of Vanadium from Spent Vanadium Catalyst from Sulfuric Acid Production. *Sci. Rep.* **2026**, *16*, 12869. [CrossRef]
95. DocsRoom—European Commission. Available online: <https://ec.europa.eu/docsroom/documents/42849> (accessed on 28 April 2026).
96. Wang, M.; Huang, S.; Chen, B.; Wang, X. A Review of Processing Technologies for Vanadium Extraction from Stone Coal. *Miner. Process. Extr. Metall.* **2018**, *129*, 290–298. [CrossRef]
97. Grzesiak, P. Utilization of industrial wastes from sulfuric acid production processes. *Przem. Chem.* **2006**, *85*, 1015–1019.
98. Pyrzyńska, K.; Wierzbicki, T. Determination of Vanadium Species in Environmental Samples. *Talanta* **2004**, *64*, 823–829. [CrossRef]
99. Liu, L.; Wang, L.; Su, S.; Yang, T.; Dai, Z.; Qing, M.; Xu, K.; Hu, S.; Wang, Y.; Xiang, J. Leaching Behavior of Vanadium from Spent SCR Catalyst and Its Immobilization in Cement-Based Solidification/Stabilization with Sulfurizing Agent. *Fuel* **2019**, *243*, 406–412. [CrossRef]
100. Bauer, G.; Güther, V.; Hess, H.; Otto, A.; Roidl, O.; Roller, H.; Sattelberger, S. Vanadium and Vanadium Compounds. In *Ullmann's Encyclopedia of Industrial Chemistry*; John Wiley & Sons, Ltd.: Hoboken, NJ, USA, 2000.
101. Sola, A.B.C.; Kumar Parhi, P.; Lee, J.-Y.; Nam Kang, H.; Kumar Jyothi, R. Environmentally Friendly Approach to Recover Vanadium and Tungsten from Spent SCR Catalyst Leach Liquors Using Aliquat 336. *RSC Adv.* **2020**, *10*, 19736–19746. [CrossRef] [PubMed]
102. Mazurek, K.; Grzesiak, P.; Trypuć, M.; Grobela, M.; Białowicz, K.; Motała, R. The comprehensive management of the hazardous vanadium catalyst waste from the oxidation of SO<sub>2</sub>; P1: Hydrometallurgical processes. *Przem. Chem.* **2010**, *89*, 253–258.

103. Wen, J.; Ning, P.; Cao, H.; Zhao, H.; Sun, Z.; Zhang, Y. Novel Method for Characterization of Aqueous Vanadium Species: A Perspective for the Transition Metal Chemical Speciation Studies. *J. Hazard. Mater.* **2019**, *364*, 91–99. [CrossRef]
104. Baldermann, A.; Stamm, F.M. Effect of Kinetics, pH, Aqueous Speciation and Presence of Ferrihydrite on Vanadium (V) Uptake by Allophanic and Smectitic Clays. *Chem. Geol.* **2022**, *607*, 121022. [CrossRef]
105. Kologrieva, U.; Volkov, A.; Krasnyanskaya, I.; Stulov, P.; Wainstein, D. Analysis of Hydrometallurgical Methods for Obtaining Vanadium Concentrates from the Waste by Chemical Production of Vanadium Pentoxide. *Materials* **2022**, *15*, 938. [CrossRef] [PubMed]
106. Wachs, I.E. Catalysis Science of Supported Vanadium Oxide Catalysts. *Dalton Trans.* **2013**, *42*, 11762–11769. [CrossRef]
107. Moskalyk, R.R.; Alfantazi, A.M. Processing of Vanadium: A Review. *Miner. Eng.* **2003**, *16*, 793–805. [CrossRef]
108. Moon, G.; Kim, J.H.; Lee, J.-Y.; Kang, J. Leaching of Spent Selective Catalytic Reduction Catalyst Using Alkaline Melting for Recovery of Titanium, Tungsten, and Vanadium. *Hydrometallurgy* **2019**, *189*, 105132. [CrossRef]
109. Jeon, J.H.; Cueva Sola, A.B.; Lee, J.Y.; Jyothi, R.K. Hydrometallurgical Process Development to Recycle Valuable Metals from Spent SCR DeNO<sub>x</sub> Catalyst. *Sci. Rep.* **2021**, *11*, 22131. [CrossRef]
110. Zeng, L.; Cheng, C.Y. A Literature Review of the Recovery of Molybdenum and Vanadium from Spent Hydrodesulphurisation Catalysts: Part I: Metallurgical Processes. *Hydrometallurgy* **2009**, *98*, 1–9. [CrossRef]
111. Lozano-Blanco, L.; Juan, D. Leaching of Vanadium from Spent Sulphuric Acid Catalysts. *Miner. Eng.* **2001**, *14*, 543–546. [CrossRef]
112. Singh, N.; Pasupuleti, K.S.; Ambili, S.; Lee, J.; Kim, M.-D.; Lee, J.-Y. Sustainable Vanadium Recovery from SAM Spent Catalysts: A Hydrometallurgical Approach for High-Purity V<sub>2</sub>O<sub>5</sub> Production and Gas Sensing Applications. *Sustain. Mater. Technol.* **2026**, *48*, e01995. [CrossRef]
113. Mazurek, K. Removal of Vanadium, Potassium and Iron from Spent Vanadium Catalyst by Leaching with Citric Acid at Atmospheric Pressure. *Green Sci.* **2014**, *16*, 59–62. [CrossRef]
114. Erust, C.; Akcil, A.; Bedelova, Z.; Anarbekov, K.; Baikonurova, A.; Tuncuk, A. Recovery of Vanadium from Spent Catalysts of Sulfuric Acid Plant by Using Inorganic and Organic Acids: Laboratory and Semi-Pilot Tests. *Waste Manag.* **2016**, *49*, 455–461. [CrossRef]
115. Sefton, V.B.; Fox, R.; Lorenz, W.P. Method of Separately Recovering Metal Values of Petroleum Refining Catalyst. US Patent US4861565A, 29 August 1989.
116. Wang, B.; Yang, Q. Recovery of V<sub>2</sub>O<sub>5</sub> from Spent SCR Catalyst by H<sub>2</sub>SO<sub>4</sub>-Ascorbic Acid Leaching and Chemical Precipitation. *J. Environ. Chem. Eng.* **2022**, *10*, 108719. [CrossRef]
117. Nikiforova, A.; Kozhura, O.; Pasenko, O. Leaching of Vanadium by Sulfur Dioxide from Spent Catalysts for Sulfuric Acid Production. *Hydrometallurgy* **2016**, *164*, 31–37. [CrossRef]
118. Marafi, M.; Stanislaus, A. Spent Hydroprocessing Catalyst Management: A Review: Part II. Advances in Metal Recovery and Safe Disposal Methods. *Resour. Conserv. Recycl.* **2008**, *53*, 1–26. [CrossRef]
119. Abbott, A.P.; Capper, G.; Davies, D.L.; Abas, F.O. Vanadium Oxide Recovery from Spent Catalysts by Chemical Leaching. *Eng. Technol.* **2008**, *26*, 1–2. [CrossRef]
120. Ho, E.M.; Kyle, J.; Lallenec, S.; Muir, D.M.; Parker, A.J. Recovery of Vanadium from Spent Catalysts and Alumina Residues. In *Hydrometallurgy '94*; Springer: Dordrecht, The Netherlands, 1994; pp. 1105–1121. [CrossRef]
121. Mousa, K.M.; Kouba, S.K. Study on Vanadium Recovery from Spent Catalyst Used in the Manufacture of Sulfuric Acid. *Iraqi J. Chem. Pet. Eng.* **2010**, *11*, 49–54. [CrossRef]
122. Mazurek, K.; Białowicz, K.; Trypuć, M. Extraction of Vanadium Compounds from the Used Vanadium Catalyst with the Potassium Hydroxide Solution. *Green Sci.* **2010**, *12*, 23–28. [CrossRef]
123. Mazurek, K.; Białowicz, K.; Trypuć, M. Recovery of Vanadium, Potassium and Iron from a Spent Catalyst Using Urea Solution. *Hydrometallurgy* **2010**, *103*, 19–24. [CrossRef]
124. Ognyanova, A.; Ozturk, A.T.; De Michelis, I.; Ferella, F.; Taglieri, G.; Akcil, A.; Vegliò, F. Metal Extraction from Spent Sulfuric Acid Catalyst through Alkaline and Acidic Leaching. *Hydrometallurgy* **2009**, *100*, 20–28. [CrossRef]
125. Erüst, C.; Akcil, A.; Gahan, C.S.; Tuncuk, A.; Deveci, H. Biohydrometallurgy of Secondary Metal Resources: A Potential Alternative Approach for Metal Recovery. *J. Chem. Technol. Biotechnol.* **2013**, *88*, 2115–2132. [CrossRef]
126. Pradhan, D.; Kim, D.J.; Ahn, J.G.; Gahan, C.S.; Chung, H.S.; Lee, S.W. Comparison of Bioleaching Kinetics of Spent Catalyst by Adapted and Unadapted Iron & Sulfur Oxidizing Bacteria—Effect of Pulp Density, Particle Size and Temperature. *Korean J. Met. Mater.* **2011**, *49*, 956–966. [CrossRef]
127. Rastegar, S.O.; Mousavi, S.M.; Shojaosadati, S.A.; Sarraf Mamoory, R. Bioleaching of V, Ni, and Cu from Residual Produced in Oil Fired Furnaces Using *Acidithiobacillus ferrooxidans*. *Hydrometallurgy* **2015**, *157*, 50–59. [CrossRef]
128. Bredberg, K.; Karlsson, H.T.; Holst, O. Reduction of Vanadium(V) with *Acidithiobacillus ferrooxidans* and *Acidithiobacillus thiooxidans*. *Bioresour. Technol.* **2004**, *92*, 93–96. [CrossRef]
129. Pourbaix, M. *Atlas of Electrochemical Equilibria in Aqueous Solutions*; National Association of Corrosion Engineers: Houston, TX, USA, 1974; pp. 1–644.

130. Santhiya, D.; Ting, Y.-P. Biobleaching of Spent Refinery Processing Catalyst Using *Aspergillus niger* with High-Yield Oxalic Acid. *J. Biotechnol.* **2005**, *116*, 171–184. [[CrossRef](#)]
131. Aung, K.M.M.; Ting, Y.-P. Biobleaching of Spent Fluid Catalytic Cracking Catalyst Using *Aspergillus niger*. *J. Biotechnol.* **2005**, *116*, 159–170. [[CrossRef](#)]
132. Zhang, J.; Zhang, W.; Zhang, L.; Gu, S. A Critical Review of Technology for Selective Recovery of Vanadium from Leaching Solution in V<sub>2</sub>O<sub>5</sub> Production. *Solvent Extr. Ion. Exch.* **2014**, *32*, 221–248. [[CrossRef](#)]
133. Vinco, J.H.; Romano Espinosa, D.C.; Soares Tenório, J.A. Purification of Vanadium-Bearing Solutions: A Comprehensive Review. *Miner. Eng.* **2025**, *227*, 109289. [[CrossRef](#)]
134. Mukherjee, T.K.; Chakraborty, S.P.; Bidaye, A.C.; Gupta, C.K. Recovery of Pure Vanadium Oxide from Bayer Sludge. *Miner. Eng.* **1990**, *3*, 345–353. [[CrossRef](#)]
135. Rokukawa, N. Resources Recycling Technology. In *Earth's 93—Recycling Congress (ReC'93). Proceedings of the International Recycling Congress, Geneva, Switzerland*; Hexagon Ltd.: Copenhagen, Denmark, 1993; pp. 14–16.
136. Kedelbayev, B.S.; Dadakhodzhaev, A.T.; Tashkarayev, R.A.; Kalymbetov, G.Y. Resource-Saving Technology for Processing of Spent Vanadium Catalysts with Vanadium Pentoxide Production and Integrated Utilization of Secondary Products. *J. Ecol. Eng.* **2025**, *26*, 258–268. [[CrossRef](#)]
137. Anioł, S.; Korolewicz, T.; Kubala, J. Investigations concerning the recovery of V<sub>2</sub>O<sub>5</sub> from the spent vanadium catalyst for the production of sulphuric acid. *Pol. J. Appl. Chem.* **1997**, *41*, 25–34.
138. Cheraghi, A.; Ardakani, M.S.; Keshavarz Alamdari, E.; Haghshenas Fatmesari, D.; Darvishi, D.; Sadrnezhaad, S.K. Thermodynamics of Vanadium (V) Solvent Extraction by Mixture of D2EHPA and TBP. *Int. J. Miner. Process.* **2015**, *138*, 49–54. [[CrossRef](#)]
139. Li, X.; Wei, C.; Wu, J.; Li, M.; Deng, Z.; Xu, H. Thermodynamics and Mechanism of Vanadium(IV) Extraction from Sulphate Medium with D2EHPA, EHEHPA and CYANEX 272 in Kerosene. *Trans. Nonferrous Met. Soc. China* **2012**, *22*, 461–466. [[CrossRef](#)]
140. Li, X.; Wei, C.; Deng, Z.; Li, M.; Li, C.; Fan, G.; Xu, H. Selective solvent extraction of vanadium over iron from a stone coal/black shale acid leach solution by D2EHPA/TBP. *Hydrometallurgy* **2011**, *105*, 359–363. [[CrossRef](#)]
141. Jiang, D.; Song, N.; Liao, S.; Lian, Y.; Ma, J.; Jia, Q. Study on the Synergistic Extraction of Vanadium by Mixtures of Acidic Organophosphorus Extractants and Primary Amine N1923. *Sep. Purif. Technol.* **2015**, *156*, 835–840. [[CrossRef](#)]
142. Toncheva, G.K.; Milcheva, N.P.; Gavazov, K.B. Liquid-Liquid Extraction-Chromogenic System for Vanadium(V) Based on 4-(2-thiazolylazo)orcinol (TAO) and Aliquat 336. *Acta Chim. Slov.* **2018**, *65*, 847–852. [[CrossRef](#)]
143. Drużyński, S.; Mazurek, K.; Białowicz, K. The use of ion exchange in the recovery of vanadium from the mass of a spent catalyst used in the oxidation of SO<sub>2</sub> to SO<sub>3</sub>. *Pol. J. Chem. Technol.* **2014**, *16*, 69–73. [[CrossRef](#)]
144. Wawrzynkiewicz, M.; Wołowicz, M.; Hubicki, Z. Vanadium(V) Removal from Aqueous Solutions and Real Wastewaters onto Anion Exchangers and Lewatit AF5. *Molecules* **2022**, *27*, 5432. [[CrossRef](#)]
145. Motała, R.; Grzesiak, P.; Grobela, M.; Hłyń, T.; Łukaszyk, J. Effect of support regeneration and active phase composition on activity of the vanadium catalysts. *Przem. Chem.* **2013**, *92*, 260–264.
146. Grzesiak, P.; Grobela, M.; Motała, R.; Mazurek, K. Effect of recovered silica on the properties of new vanadium catalysts. *Przem. Chem.* **2010**, *89*, 372–376.
147. Grzesiak, P.; Grobela, M.; Motała, R.; Mazurek, K. Opracowanie metod odzysku krzemionki ze zużytych katalizatorów nie posiadających zdefektowanej tekstury nośnika [Development of Silica Recovery Methods from Spent Catalysts without Defective Carrier Texture]. In *Kompleksowe Zagospodarowanie Szkodliwych Odpadów Katalizatora Wanadowego Stosowanego do Utleniania SO<sub>2</sub>*; Trypuć, M., Grzesiak, P., Mazurek, K., Grobela, M., Eds.; Wydawnictwo Naukowe Instytutu Ochrony Roślin w Poznaniu: Toruń-Poznań, Poland, 2009; Volume 2, pp. 195–219. (In Polish)

**Disclaimer/Publisher's Note:** The statements, opinions and data contained in all publications are solely those of the individual author(s) and contributor(s) and not of MDPI and/or the editor(s). MDPI and/or the editor(s) disclaim responsibility for any injury to people or property resulting from any ideas, methods, instructions or products referred to in the content.